IU B International University Bremen

Downstream Processing of Natural Products: Carminic Acid

by

Rosa Beatriz Cabrera

A thesis submitted in partial fulfilment
of the requirements for the degree of
Doctor of Philosophy

Approved Thesis Committee

Prof. Dr. H. Marcelo Fernandez-Lahore

Prof. Dr. Georgi Muskhelishvili

Prof. Dr. Osvaldo Cascone

Prof. Dr. Mathias Winterhalter

School of Engineering and Science

26th May 2005

Downstream Processing of Natural Products:

Carminic Acid

NOTE FROM THE AUTHOR

Bioprocessing industries increasingly require overlapping skills coming from various disciplines. For products to move form the laboratory to the market demands more than an understanding of biology. Nowadays, understanding of the fundamentals of chemical engineering and their application to large-scale product recovery and purification is a key competitive advantage. The hybridization of the biochemist and the chemical engineer created a new discipline that of bioproduct process designer. When applied to product recovery and purification this is commonly referred as Downstream Processing.

This work has been developed in cooperation with an industrial partner interested in the downstream processing of carminic acid, as a natural food colorant. Therefore, some details of the work are not presented here nor published in the open literature since they are considered as industrial secret.

Experimental work was performed at both the University of Buenos Aires (Argentina) and the International University Bremen GmbH (Germany). Pilot plant studies were performed at Naturis S.A., Buenos Aires (Argentina).

ABSTRACT

Carminic acid (E 120) is a natural colorant extracted from cochineal e.g., the desiccated bodies of *Dactylopius coccus* Costa female insects. The major usage of Natural Red lies in the food, cosmetic and pharmaceutical industries. The recovery and purification of carminic acid from raw cochineal is regarded as a difficult and complicated process. Current industrial technology suffers from low and irreproducible yields while generating a low quality final product.

An improved strategy for the downstream processing of carminic acid was developed. Beaded adsorbents were screened and subsequently tested in packed-bed and finite bath contactors. Efficient adsorption and desorption conditions were found for two resin types. Depending on the physical nature of the solid supports employed, different mass transfer resistance mechanisms were identified. Fluid side effects and intraparticle resistance mechanisms were dominating. This was quantitatively described in terms of film mass transport coefficients and particle diffusivities e.g., a conventional solid diffusion or pore diffusion coefficients. Employing batch adsorption in an agitated vessel in combination with a macroporous beaded adsorbent showed a dramatic increase in sorption performance as a function of the fluid regime in the vessel. A hybrid mechanism including a perfusion like component can be hypothesized in order to explain these experimental findings. Quantitative evaluation of these events required the definition of a modified pore mass transfer coefficient or *hyperdiffusivity*, which is able to account the influence of mixing on sorption kinetics.

The knowledge generated served as the basis for the design of an adsorption process at the pilot scale. This process is amenable for direct capture of the product after optimized cochineal extraction without previous extensive clarification. Moreover, the process yielded a high quality carminic acid preparation. The final product complied with food industry regulations and it was free of toxic metal ions and allergenic components. Process productivities compared favorably with current manufacturing schemes. General criteria for further scale-up are provided.

ACKNOWLEDGMENTS

In order to obtain my PhD degree I moved 1,000 kilometers from my hometown, and in some way I finished 5 years later, in another language and about 12,000 kilometers away from there. Thus, I have much more than a PhD thesis. I could not have finished this project without the help of a lot of people whom influenced me greatly. One of the pleasures of finally finishing is the opportunity to thank them.

First of all, I must express my great gratitude towards my advisor, Dr. Marcelo Fernandez Lahore who gives me the opportunity to work in Downstream Processing starting from the scratch because of my previous scientific background. He fed my ego every day and always blames my bad results to my inexperience and not to my ignorance. I always appreciate his confidence in me, his understanding, patience, knowledge, skills, and his assistance in writing reports all this years. He gave me a direction, technical support and became a friend besides being my mentor and professor.

I would like to thank all the people of the laboratories of "Industrial Microbiology and Biotechnology" of the Biochemical Faculty of University of Buenos Aires, whom received me five years ago and from whom I learned much more than Biotechnology: Dra. Ana Giulietti, Dr. Osvaldo Cascone, Dra. Clara Nudel, Dr. Mariano Grasselli, Dra. Victoria Miranda, Dra. Silvia Camperi, Lic.Agustin Navarro del Cañizo. I want to thank the rest of my lab mates Federico, Laura, Nancy, Mariela, Juliana, Francisco, Natalia, Carolina, Mercedes, Lucas, Virginia, Gustavo for all their conversations, their friendship and tolerance. To Alejandro who is always cheerful and

willing to eat something, drink mate or "teres", share a joke or just talk with me. Thanks also goes out to other PhD, professors, and assistances, Rodrigo, Alejandra, Particia, Cecilia, Walter, Julian, Susana, Edy, Malena, Isabel and to everybody whom I could not mention here.

Very special thanks go out to my "residents family" in the apartment in UBA. With them it was very easy for me to live so fare away from my home: Juliana, Cecilia, Ana, Jose, Kathy, Caro, Chango, Ines, Angeles, and specially to Luciano with which the destiny caused that we crossed our ways already several times in our life, and now I do not know in what paragraph I must include it.
Thanks also to my friends Marcelo, Ricardo, Lorena, Maria, Silvina, Laura, Martin, Guiye, Horacio and particular for Cecilia (my sister of soul) who is still my best friend after 21 years, to her… *my "big backpack" not necessarily is full and it is not easy to fill it.*

To the people of the International University of Bremen for giving me the opportunity to live in Germany, in another culture and paradoxically to learn more about my culture and about myself. Especially to my colleagues of the laboratory of Downstream Processing: To Sabine for her help and tolerating me every day.

Thanks to Georgi Muskhelishvili and Mathias Winterhalter to have accepted to read and to correct my work. To Georgi great group: Nico, Claudia, Ramesh, Michi, Sebastian, and Marcel for their company, friendship and the coffee.

A special recognition to my family, which, close or far away, always has been with me as I have been with them. Especially to my mother, Eva, that has been strong enough to let me go of her side,

believe in me, accept and to respect my necessity of freedom. To my brother, Juanchi and its family, and to the memory of my father, Juan, who would be proud of me.
An finally, to Marcel, for his loving support, staying with me always and to do that I smile every day. *Te amo.*

In conclusion, I recognize that this research would not have been possible without the financial assistance of R&D Grant (2002-2003). National Agency for the Promotion of Science and Technology. Buenos Aires (Argentina). Industrial partner, Naturis S.A. And to the financial assistance of International University Bremen.

INDEX

ABREVIATIONS

Notation

Abbreviations

AOAC	Association of Analytical Communities
CA	Carminic Acid
FAO	Food and Agriculture Organization
IUPAC	International Union of Pure and Applied Chemistry
LAPU	Leucine aminopeptidase unit
WHO	World Health Organization

Symbols

B	Solid concentration [$\%w \cdot w^{-1}$]
Bi	Biot number [-]
C	Liquid-phase adsorbate concentration [$kg \cdot m^{-3}$]
D_{AB}	Diffusion coefficient in free solution [$m^2 \cdot s^{-1}$]
d_c	Column diameter [m]
D_i	Diameter of impeller [m]
D_{pm}	Modified pore diffusion coefficient [$m^2 \cdot s^{-1}$]
D_p	Pore diffusion coefficient [$m^2 \cdot s^{-1}$]
d_p	Particle diameter [m]
D_s	Solid diffusion coefficient [$m^2 \cdot s^{-1}$]
D_T	Tank diameter [m]
g	Gravity acceleration [$m \cdot s^{-2}$]
k_1	Adsorption rate constant [$l.g^{-1} \cdot s^{-1}$]
K_d	Langmuir isotherm constant [$kg \cdot g^{-1}$]

K_F	Freundlich isotherm constant [$kg \cdot g^{-1}$]
k_f	Film mass transport coefficient [$m \cdot s^{-1}$]
M	Molecular weight [kDa]
n_c	Critical stirrer speed [$r \cdot s^{-1}$]
N_i	Impeller rotational speed [$r \cdot s^{-1}$]
q	Solid-phase adsorbate concentration [$g \cdot kg^{-1}_{adsorbent}$]
q_m	Maximum capacity [$g \cdot kg^{-1}_{adsorbent}$]
q*	Equilibrium capacity [$g \cdot kg^{-1}_{adsorbent}$]
Re_i	Impeller Reynolds number [-]
Re_p	Particle Reynolds number [-]
Sc	Schmidt number $\eta/(D_{AB}.\rho_l)$ [-]
T	Absolute temperature [K]
U	Linear superficial velocity [$m \cdot s^{-1}$]
V	Liquid-phase volume [m^3]
w	Mass of adsorbent [kg]

Subscripts

o	Initial
f	Final
e	Equilibrium
max	Maximum

Geek letters

δ	Delta parameter [-]
η	Dynamic viscosity [$kg \cdot m^{-1} \cdot s^{-1}$]
ε	Extinction coefficient/ interstitial volume
ε_p	Intraparticle porosity

μ	Ionic strength
ν	Kinematic viscosity [$m^2 \cdot s^{-3}$]
ρ_l	Liquid density [$kg \cdot m^{-3}$]
ρ_p	Solids density [$kg \cdot m^{-3}$]

1. INTRODUCTION

1.1. Food Natural Colorants

Appearance of food is as important as its taste and therefore modern food manufacturers have become greatly concerned with conserving the aspect of foods, which may have lost their natural colors during processing. The addition of colorants preserves the aspect of foods while also reduces batch-to-batch color variations and enhances its acceptance by the consumer. However, synthetic colorants are currently perceived as undesirable or harmful [2] [3, 4]. Moreover, the European Union and the United States have restricted the use of synthetic colorants as food additives [5]. These restrictions have increased the use of natural colorants in the food industry.

Carminic acid is a natural colorant [6] that is extracted from the bodies of *Dactylopiidae* female insects i.e. cochineal. These insects are sessile organisms living on *cactaceae* (*Opuntia sp*). The *prickly pear* cacti are found in the semi-arid areas of Peru, Bolivia, Chile, the Canary Islands (Spain) and Mexico. Carminic acid is the principal pigment in the cochineal. The major usage of this colorant today lies in non-textile applications, like cosmetics, foods, and pharmaceuticals.

1.2. Chemistry

Carminic acid is the 7 - α - D – Glucopyranosyl - 9,10 – dihydro -3, 5, 6, 8 tetrahydroxy-1-methyl-9,10-dioxo-2-anthracene-carboxylic acid, according to the IUPAC nomenclature system (Figure 1). This compound is an anthraquinone glycoside and contains several acid centers; the first dissociation step occurs at carboxylic group in the position 2 (pK_0=2.9), which is the most acidic site. The following acid-base equilibrium (pK_1=5.4) involves the 6-hydroxyl group since the 5- and 8- OH groups (pK_2=8.7 and pK_3=12.2) are less acidic due to their position with respect to the carbonyl, which reduce the hydrogen mobility through hydrogen bonding [7].

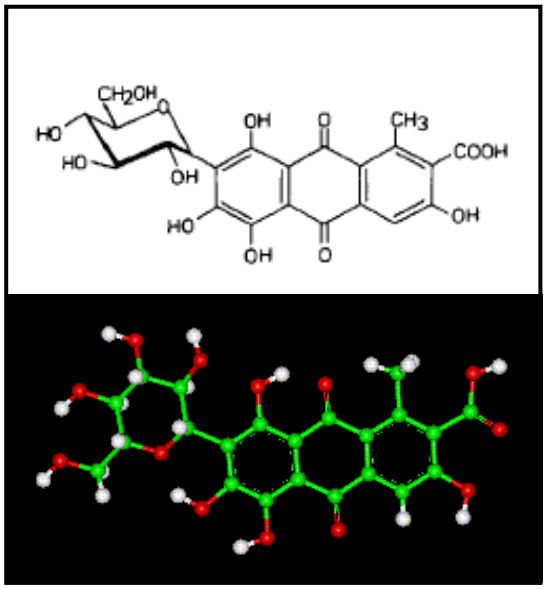

Figure 1: Molecular structure of carminic acid.

Important for technological applications carminic acid is soluble in water. These solutions had little intrinsic color below pH 7, where the quinone ring has greatest photo stability, showing at pH near 4 a pale-straw tint. Also important is the property of forming complexes with several metals ions. Complexation shifts the maximum absorption in the

Figure 2: Carminic acid solution at different pH (7 – 5 –4 and 3).

visible range to higher wavelengths, with an apparent increase in color intensity when viewed by naked eye. The most brilliant colors are produced with aluminum (Figure 2).

Carminic acid is insoluble in petroleum ether, benzene and chloroform. It fuses at 135ºC but can be decomposed by heat treatment (80ºC, 1 h) [8].

Common name	Carminic acid, Cochineal, Carmine
C.I. number	75470
C.I. name	Natural red 4
Class	Natural E120
Ionization	Acid
Solubility	Soluble in water and ethanol
Absorption maximum	494 (0.02N HCl)
Color	pH variable (orange – violet)
Empirical formula	$C_{22}H_{20}O_{13}$
Formula weight	492.39

Table 1: Carminic acid properties.

1.3. Biology

The superfamily *Coccoidea*, commonly known as *cochineal insects*, *mealybugs*, or *scale insects*, are hemipterous insects, which constitute a homogeneous and specialized group of small phytophagous insects. They are also characterized by a high degree of adaptation to the parasitic life and show extreme sexual dimorphism (Figure 3). The family *Dactylopiidae* (carmine cochineals) is found exclusively on cacti. Female insects are sessile organisms, which usually form colonies feeding externally on cladodes. These insects are 3-5 mm in length and are easily identified by the presence of a white cotton-type wax secretion that covers the red purple body. Dactylopiidae consists of a single genus, *Dactylopius*, including nine species. The family contains the commercial carmine cochineal (D. *coccus* Costa) which is the basis of the cochineal dye industry and which is reared for commercial purposes on the cactus *Opuntia ficus-indica* (L.) Mill (Figure 4) [9] [1].

Fully developed females weight is around 45 mg losing ca. 70% on drying. The concentration of pigment is highest when

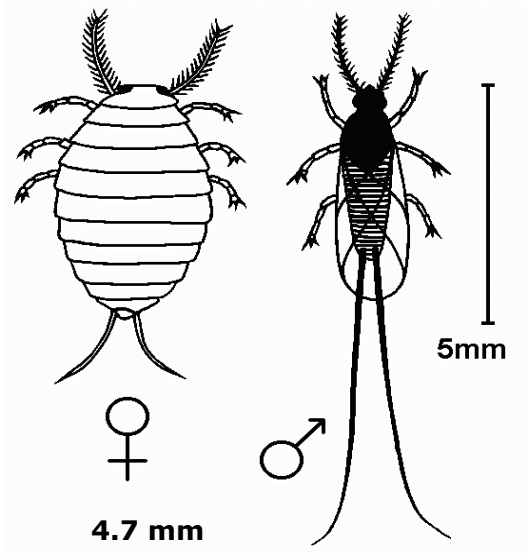

Figure 4 Homeoptera: Coccidae: Dactylopius sp.[1].

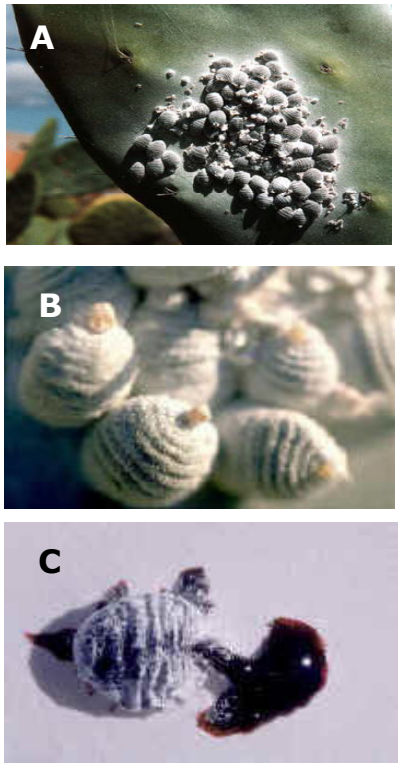

Figure 3: A-B) Female cochineal insects on *Opuntia* sp., C) squeezed female body.

the female insects are sexually mature, at an age of 90-120 days, just before egg-laying begins. Indeed, on dissection and microscopic examination of freshly collected specimens highest concentrations of the color appear to be associated with the egg yolk. This is to be incorporated later into the tissues of the embryo and it is presumed that the colorant biosynthesis continues during the remaining phases of the development of the organism [10].
Biosynthetic mechanisms of carminic acid are largely unknown [9]. The compound might have defense or deterrent functions towards natural predators [11].

1.4. History

The Cochineal insect is native from Mexico, Central America and Peru. There is evidence of its use since the tenth century. The Aztecs called it *nocheztli* that means blood of tuna. Various studies have shown that tunics and gowns were dyed with cochineal at the pre-Columbian times [12].

Spanish conquers were fascinated by the intense scarlet color of cochineal dye, which was brighter and better than any known European dyestuffs in the sixteen century. In fact, after gold and silver, cochineal becomes one of the most demanded import commodities from Central-America.
By the seventeenth century the production of cochineal was unsuccessfully attempted in Europe while promoted in the Spanish colonies. Therefore, this industry early played an important role in the economic development of Central and South America.

Due to its commercial value by the nineteenth century cochineal *plantations* were introduced in many parts of the world e.g., the Canary Islands, Australia, South Africa, Bostwana, Nepal, India and Sri Lanka [13]. Despite of this, the greater economic profit in the culture of cochineal outside America was restricted to the Canary Islands. Exports of the dried insects rose from a few kilograms in 1831 to over 3000 tones in 1875. Small amounts of high quality cochineal are still available from the Canary Islands today.

With the appearance of synthetics aniline derived colorants in approx. 1950 the demand and commercialization of the natural colorants was progressively reduced. Nowadays, and due to the carcinogenic and toxic effects described for those compounds, the interest in employing natural colorants has resurged. Cochineal and their derivatives are already approved by the United State Food and Drug Administration (FDA) and are currently accepted for industrial uses. Carminic acid is used in cosmetics and in the food sectors. France, the United Kingdom, USA, Japan, and Argentina are the main markets today. Peru remains the world's largest producer of raw cochineal with annual yields in the range of 300 – 900 tones. Attempts are being made to increase cochineal cultivation or industrial processing in other Latin-American countries i.e., Mexico, Chile and Argentina.

1.5. Cochineal production

1.5.2. Agronomical and primary processing aspects

Harvesting of the cochineal insects is still undertaken by hand and involves brushing the white-gray, powdery mass of females off the plant immediately prior to egg laying. Primary processing involves killing the organisms and drying the insect bodies. Simple sun drying of the insects provides *silver cochineal*, which includes the brood powder and is regarded as of inferior quality. Accelerated, artificial killing and drying gives the more highly graded *black cochineal*; a brief immersion in hot water followed by sun drying is the commonest method. Between 80,000-100,000 insects are required to produce one kilogram of raw dried cochineal as exported. Cultivation yields in Peru have been reported to range from 120 – 240 $kg \cdot ha^{-1} \cdot year^{-1}$.

Figure 4: Harvesting of the cochineal.

Figure 4: A) "silver cochineal"; B) "Black cochineal" .

Exporters normally undertake cleaning and grading. This usually involves removal of extraneous matter by manual sieving and sieving and re-drying, if necessary, to 12% moisture content. Some reports in the literature state that in Mexico and Central America a distinction is made between

cultivated and wild strains of insects. The former is larger and contain more pigment (up to 21-22% (w/w) on dry basis). Wild type insects in Peru regularly contain at least 16% (w/w) carminic acid [6]. First class cochineal is defined as the material retained by #10-#14 sieves [14].

1.5.3. Industrial processing

The downstream processing (i.e., recovery and purification) of carminic acid from raw cochineal is regarded as a difficult and complicated process [15].
Current industrial manufacture practices are derived from a traditional precipitation procedure, based on complex formation with metallic ions. This strategy possesses many disadvantages and is unable to deliver a safe, highly purified product with high yields [16]. According to the Canadian International Development Research Center (IDRC) standard industrial cochineal processing is a multiple step procedure consisting in the following operations [17]:

a) Treatment of the sieved cochineal with organic solvents (e.g., hexane) to remove waxes and lipids
b) Milling to an appropriate particle size e.g., 100 mesh
c) Alkaline extraction
d) Solid-liquid separation e.g., flocculation and filtration
e) Insoluble lake formation with aluminum and calcium salts
f) Recovery of the precipitate e.g., centrifugation
g) Resolubilization of carminic acid
h) Concentration
i) Formulation

The details on actual commercial procedures used by individual manufacturers are jealously guarded as trade secrets [9]. However,

these processes are known to be characterized by low yields (< 52%) and usually provide low quality products. They also suffer form a lack of robustness, instability due to multiplicity of operational factors, and are non reproducible. These facts contribute to the generation of batch-to-batch inconsistencies and overall increased processing costs. Incorporation of varying amounts of toxic metal ions and allergenic proteins to the final carminic acid preparation is common. This may have a negative impact on consumer health.

1.5.4. Production chain and product added value

Primary production, industrialization, and commercialization of carminic acid is characterized by four key economic activities which contributes to the overall added value chain, as follows:

- Source of primary production (e.g., country)
- Classification and storage activities
- Industrialization to final product
- Distribution and commercialization

Among these the most critical step regarding the value added to the final product is the industrialization. This consists mainly in the downstream processing of carminic acid from raw cochineal to the final preparation. As it is the common situation in the production of natural products, the purification process makes up a major part of production cost. For example, carminic acid sold as a lake has a value that is 8 times higher than the same product sold as cochineal. This factor is enhanced in the case of highly purified carminic acid preparations.

1.6. Cochineal and derived commercial products

1.6.1. Quality standards

The *Instituto de Investigación Tecnológica Industrial y de Normas Técnicas del Perú* (ITINTEC) has established quality standards for commercial cochineal: Carminic acid content (min. 17.5%), humidity (max. 13%), lead concentrations (max. 3 ppm), and pH (5.0-5.6). The same Institution jointly with the Committee of Experts FAO/OMS for Food Additives (JECFA) proposes analytical techniques for evaluating the pigment in cochineal samples (FAO/OMS, 2000)[6].The European Parliament and the council of the European Union specifies the main use and limits for each foodstuff (soft drinks 100 $mg \cdot L^{-1}$ and in solid food 50-500 $mg \cdot kg^{-1}$) [18]. In Japan, carminic acid rather than carmine is employed by the food industry (refer to commercial products).

1.6.2. Safety data

Cases of adverse reactions to cochineal products were reported after occupational exposure, dermal contact, or consumption. Allergic reactions were demonstrated although allergens are not fully identified [19-21]. However, insect-derived proteins (possibly complexes with carminic acid) might be responsible for IgE-mediated allergy to carmine [19]. Criteria for inclusion of carmine products as allergenic food are not satisfied. The European Parliament and the council of the European Union recommend a restriction of protein level in E 120 [18]. The FDA (1999) indicates that carmine derived colorants must be treated to assure the absence of *Salmonella*.

1.6.3. Commercial products

1.6.3.1. Cochineal extract

The extract of cochineal is a concentrated solution obtained after eliminating the ethyl alcohol of the watery-alcoholic extract of cochineal dried insect bodies [5], [15]. It presents good light stability; it has a color that varies from orange to red, depending on pH. The raw cochineal extract is frequently stabilized with citric or tartaric acids. According to the specifications of the FDA (1999), the cochineal extract must comply with the following specifications: pH 5.0-5.5; carminic acid content: min.1.8%, total solids: 5.7- 6.3%, total protein: 2.2% max., lead: 10 ppm max., and arsenic max. 1 ppm. The cochineal extract finds application as food colorant in yogurts, soft drinks and alcoholic beverages.

1.6.3.2. Carmine

Carmine corresponds to the lake of carminic acid, prepared by precipitation with Al^{2+} or Ca^{2+}. The final color of the product will depend on the proportion of aluminum and calcium, being violet in formulations without calcium and varying from pink to scarlet as it increases the proportion of calcium. Depending on pH, color varies from red ($pH < 4$) to blue-red ($pH \approx 10$). This preparation is stable to light, temperature and oxygen exposition. It is soluble in alkalis and insoluble in acids. The carminic acid concentration varies between 40% and 65%, being carmine 50% the one of greater commercial importance [22]. According to the FDA (1999) carmine must satisfy: carminic acid content min. 50% w/v, lead max.10 ppm, and arsenic max 1 ppm. Carmine is used as and additive colorant in the dairy industry for yogurts, ice creams and milk-based beverages. In the

meat industry is pre-dispersed in sausage mass and the like. It is also used in sweets, filled candies, fruit conserves, and bakeries.

1.6.3.3. Carminic acid

Pure carminic acid is commercialized as powder or as solutions with concentrations ranging from 1 to 10% (w/v). Purity levels are between 50-60% [6]. Spray dried preparations are also available with a 2-7% carminic acid content. Carminic acid competes with beetroot red (betanin) and anthocyanins in food coloring and its main limitation is insolubility at low pH. To this end, many manufactures let carminic acid further reacts with ammonia in order to obtain acid-stable carmine [23]. Food applications include soft and alcoholic beverages, marmalades, cake dry mixtures and conserves. Carminic acid also finds applications in pharmaceutical and cosmetic industry, as textile dye, pH indicator, and histological stains.

1.7. Economy

Cochineal is produced in a few countries worldwide. Peru is the world main producer (78%) followed by Chile (17%) and the Canary Islands (1.5%). Advanced agricultural techniques and genetic improvement is nowadays employed for cochineal production although small-scale producers based on wild-type *D. coccus* recollection still are present. Others countries producing cochineal are Mexico, Bolivia, Argentina and South Africa but they account for only 10 Ton·year^{-1}[24]. Traditional exports were based on raw cochineal but nowadays a processing industry is under development. Major cochineal importers are Europe (e.g., Germany, Italy, France, UK, Spain), the USA, Japan, and Argentina [6].

Increased availability of raw material has led to a progressive reduction in FOB export prices from around US$ 50/kg and US$ 250·kg^{-1} for cochineal and carmine, respectively, to US$ 17/kg and US$ 100·kg^{-1} in the few last years. The current price levels are of a similar order of magnitude to those prevailing in the mid-1970s. The global consumption of cochineal and carmine has been substantially increasing due to price stability and a trend towards the use of natural colorants in foodstuffs.

1.8. Downstream processing of natural products

Naturals products have been known and exploited for many purposes for example, as food additives or as pharmaceutical preparations. They were formerly used as raw extracts with minimal processing. A current requirement for higher standardizations implies the need for concentration, selective isolation and purification of active components from the crude mixtures.

The field of downstream processing of these natural products has been characterized by the existence of a pool of knowledge shared between the practitioners. This pool of knowledge is usually unavailable in the open scientific or patent literature. Therefore, theory has generally followed behind general practice and many techniques and observations, which are truly state of the art, are not easily available. With the increasing sophistication of the processing industries, procedures have been rationalized in terms of scientific principles. But still, as any one time, there exists an accumulation of wisdom among experienced practitioners that is difficult to access from the usual academic source.

The art, science, and practice of downstream processing synthesize the knowledge of the biochemist and the principles of chemical engineering for improved natural product recovery and purification. A wide variety of methods and techniques are therefore employed. It is the task of the downstream processing scientist to make the correct choice and efficiently apply the current state of the art in each technique to match the success of modern bioprocess technology [25]. A typical processing profile includes a number of distinct unit operations, like extraction or isolation, concentration or dewatering, coarse fractionation or recovery, high-resolution purification, polishing, and formulation. Figure 5 illustrates the processing scheme for enzyme manufacturing. The use of a large number of sequential unit operations necessary to achieve the desired purity of a product heavily contributes to the overall processing costs. Moreover, this situation is responsible for reduced product yields [26]. This has lead to the introduction of the so-called *integration* concept where new and efficient unit operations are designed and implemented, thus limiting the total number of processing steps, increasing product yields, and contributing to cost effectively.

The overall performance of a purification process, expressed by its overall yield, operation time, and capital cost may contribute to up to 70-90% of the total production costs for a biological product. As was stated before, a reduction in the number and the effective sequencing and dovetailing of unit operations during the recovery and purification train strongly influences the economic success of a potential product [27, 28]. Figure 6 depicts the relationship between selling price and processing extent required for the manufacturing of various biotechnological products in the market. Carminic acid is found here closer to other organic molecules like antibiotics, aminoacids, and other metabolites.

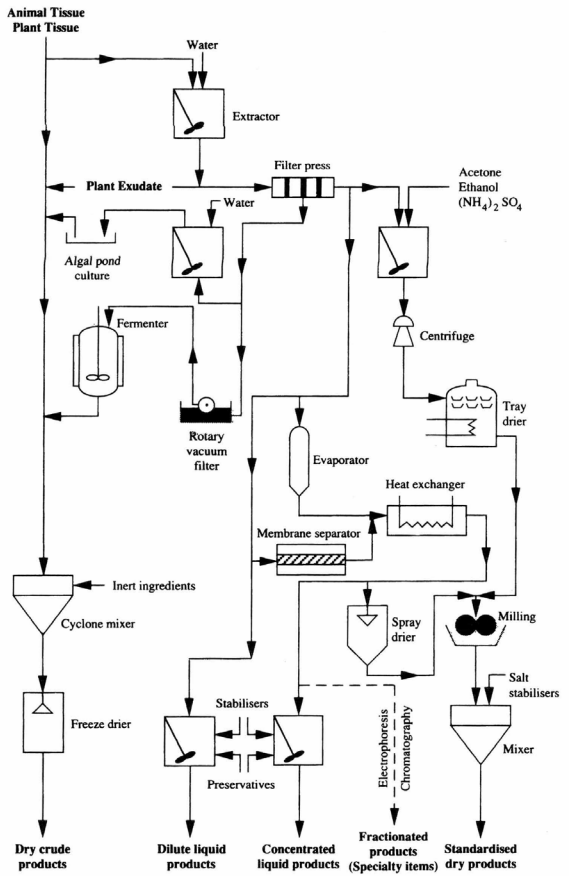

Figure 5: Unit operations used in the manufacture of enzymes [29].

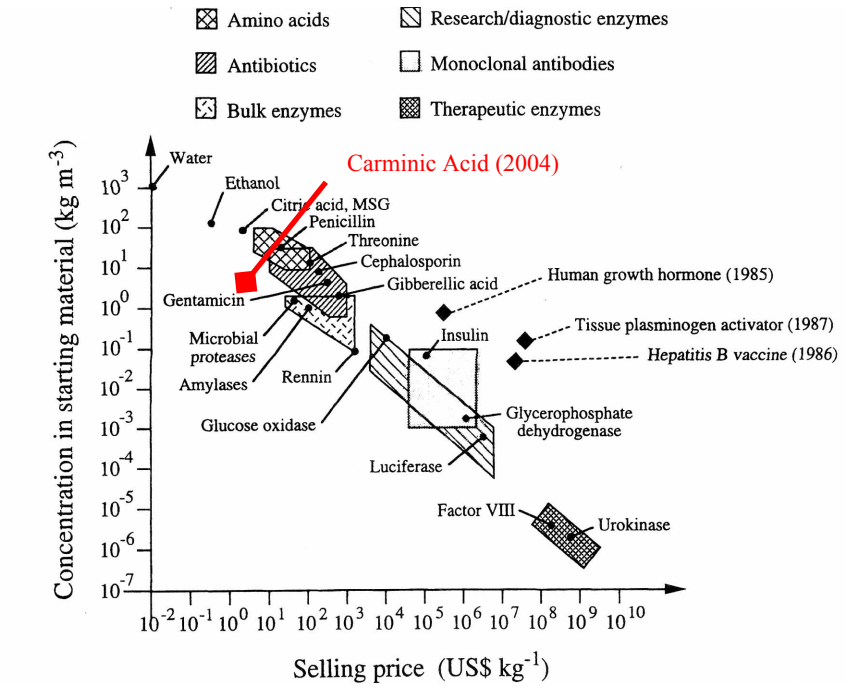

Figure 6: Relationship between selling price and concentration before downstream processing for several products [29].

A powerful technique commonly employed in downstream processing is the capture of a soluble product onto a solid phase e.g., a beaded support. To be selective, such processes typically exploit significant differences between products and unwanted impurities expressed as a general molecular character, like charge, hydrophobicity, size, and affinity. Competitive industrial application of adsorption strategies demands the innovation of cheap, nontoxic, and easily available adsorbents. Moreover, definition of kinetic parameters and adsorption characteristics are of prime importance for efficient process design, modeling, and scale-up. The parameters characterizing the mechanisms involved in the adsorption and desorption stages, as well as, the different operational modes e.g., finite bath, packed-bed or fluidized-bed could be estimated from proper correlations and/or by matching the predictions of appropriate models, which are developed to describe the behavior of the adsorption in the different stages and operational modes, with experimental data. Theoretically calculated numbers from correlations or experimentally derive parameters from regression analysis can be integrated into mathematical models that would satisfactory predict the behavior of the adsorption stages under different operational modes. Furthermore, these models could be used in the complex tasks of design, optimization, control and scale-up the adsorption processes [30].

A definite advantage of employing direct adsorption methods is their capability to handle crude extracts containing suspended biological particles without previous clarification. Simultaneous concentration and selective isolation of a defined product from a raw extract becomes then a viable strategy. Further elution and formulation would complete product delivery to its final form. This strategy is proposed for the

downstream processing of carminic acid from cochineal. It is expected that an integrated design will favorably compared with the traditional process currently found in the carmine processing industry.

2. OBJECTIVE

The main goal of the present work was to develop a novel strategy for efficient downstream processing of carminic acid, a valuable natural colorant, from raw cochineal. The product is intended as a safe, high quality, food additive. In order to accomplish this general goal several partial objectives were defined, as follows:

- *To design an adsorption-based process fulfilling the criteria for implementation at an industrial setting in terms of product quality, process robustness and scalability, process overall productivity, and cost.*

- *To run laboratory scale experiments for screening, optimization, and quantitative characterization of the process*

- *To design and to evaluate an appropriate process for carminic acid production at the bench scale*

- *To study the process performance at the pilot scale*

- *To define scale-up criteria*

3. MATERIALS AND METHODS

3.1. Materials

First class Peruvian cochineal (21-22 % carminic acid content) was provided by NATURIS S.A. (Victoria, Buenos Aires, RA). Beaded adsorbents were obtained from Biosix S.A. (Buenos Aires, RA). Flavourzyme was purchased from Novozymes A/S (Bagsvaerd, DK). Carminic Acid (7-C-D glucopyranosyl – 3, 5, 6, 8- tetrahydroxy – 1 - methyl- 9, 10 –dioxo – 2 - anthracenecarboxylic acid) was from Sigma-Aldrich Chemical Co. (St. Louis, MO, USA). All other chemicals were of analytical grade (Fluka, Buchs, CH). Process solvents and chemicals were provided by Anedra S.A. (Buenos Aires, RA). The ODS Supelco column (4.6 mm x 15 cm, 5 μm packing particle diameter) was from Sigma-Aldrich Chemical Co. (St. Louis, MO, USA).

3.2. Methods

3.2.1. Process analytics

Spectral scan: The carminic acid spectrum was obtained by scanning a solution of pure carminic acid in HCl 0.02 N in a Shimadzu UV-1700 spectrophotometer (Shimadzu Corp., Duisburg, Germany).

Determination of carminic acid: The spectrophotometric method described by the Instituto de Investigación Tecnológica Industrial y de Normas Técnicas de Perú (ITINTEC) and the Joint FAO/WHO Expert Committee on Food Additives (JECFA) was employed. A modification of this procedure was used for the analysis of large number of samples during adsorption experiments (modified VIS method). Briefly, carminic acid concentration was determined after diluting each sample

(1:100, HCl 0.02 N) by visible absorption at 494 nm. Determination of the pigment concentration was done in duplicate, according to Lambert and Beer law:

$$CC\ (g \cdot L^{-1}) = \frac{A \cdot f \cdot 492.39}{5800} \qquad \textbf{Equation 1}$$

Where **A** is the absorbance of the sample diluted in HCl 0.02N at 494 nm; **f** is the dilution factor, **492.39** is the carminic acid molecular weight ($g \cdot mol^{-1}$) and **5800** is the (ε) extinction coefficient ($mol^{-1} \cdot cm^{-1}$ in HCl 0.02 N). Carminic acid was determined also by an isocratic HPLC method (Hewlett-Packard HP 1090, Waldbronn, Germany) using a ODS column irrigated with a mobile phase consisting of methanol 60 mM phosphate buffer pH 6 (20:80) at a flow rate of 1.2 $ml \cdot min^{-1}$. Detection was performed at 220 nm, 280 nm, and 560 nm. Sample was injected using a manual Reodyne (Cotati, CA, U.S.A) valve (20 μl loop).

In adsorption processes, the supernatants were most often taken as the samples for the determination of the residual carminic acid concentration. The amount of carminic acid was then obtained from the system material balance:

$$q = \frac{V}{W} \cdot (C_0 - C) \qquad \textbf{Equation 2}$$

Where ***q*** is the amount of carminic adsorbed per unit of adsorbent mass ($g \cdot kg^{-1}$), ***V*** is the volume of liquid phase (L), ***W*** the adsorbent mass (kg), $\boldsymbol{C_0}$ is the carminic acid initial concentration in the feedstock, and ***C*** is the carminic acid concentration in solution ($g \cdot L^{-1}$).

Total protein determination. The Compat-Able Protein Assay Preparation Reagent Kit and the BCA Protein Assay Kit (Pierce, Rockford, IL, USA) were employed, according to manufacturer instructions [31].

pH and Conductivity. A PP50 pH/ATC meter (Sartorius, GÖttingen, Germany) provided with a combined pH electrode and a conductimeter probe was used, following the manufacturer instructions.

Process fluid density. Density was determined using a pycnometric technique, employing standard procedures [32].

Process fluid viscosity. The viscosity was measured employing the Ostwald viscosimeter following the instrument manufacturer instructions (Schott-Geräte GmbH, Mainz, Germany).

Dry weight. Moisture is expressed as a percentage of the dry weight of material. The sample was dried in a vacuum oven at 105°C and dried to a constant weight for 5 hours according to the AOAC methods 926.08 and 925.09 (1990). The moisture loss was determined gravimetrically [33].

3.2.2. Aqueous cochineal extract

Milled or intact cochineal was employed for extraction experiments. These were typically carried out in Erlenmeyer flasks (5 g of finely ground cochineal in 100 ml of extract solvent; 1:20) by shaking (100 rpm) at 95ºC. Water, 50 mM ammonium acetate buffer (pH 6), 0.1% Triton X-100 in water, 1 M HCl, and 0.5% NaOH were used as extractive solvents. The enzymatic treatment was performed by adding

2 g of neutral protease (500 LAPU·g^{-1}) per 100 g of alkaline extracted cochineal, at 50ºC with stirring for 16 h.

Other parameter relevant to extraction were explored using 50 mM ammonium acetate buffer (pH 6):

a) The effect of temperature was studied in the range between 5 and 100ºC at time intervals between 10 and 60 min.
b) The influence of extractant volume on the recovery of carminic acid was explored at 1:5, 1:20, 1:40, and 1:100 solids to solvent ratios.
c) The efficiency of sequential extraction was also studied employing a 1:20 solid to liquid ratio and 1, 2, 3, and 4 solvent contacting steps.

The optimized protocol for preparation of the crude extract was performed as follows: 1 kg of finely ground cochineal was treated with 0.15 M NaOH (5 L) at 90°C for 20 min., and subsequently diluted with 10 L of distillated water. Heating was continued for additional 20 minutes under stirring. Finally, the extract was sieved to eliminate coarse cochineal particles using a mesh count. The resulting cake was further washed with demineralised water (5 L, 90°C). The final solid-to-liquid ratio was 1:20, the final ionic strength not exceeded 7 ms·cm^{-1}, and pH was in the range of 5.5-6.5.

3.2.3. Conditioning of the adsorbent materials

The ion-exchange resins were activated by sequentially contacting the solids with 10 volumes of the following: a) 0.1 N NaOH, b) water, c) 0.1 N HCl. Finally, extensive washing with distilled water was performed until pH 7 was reached in the eluent. The resin was then equilibrated with 50 mM ammonium acetate buffer, pH 6. Soft gel and ceramic base materials were equilibrated in running buffer without previous treatment.

3.2.4. Adsorbent screening

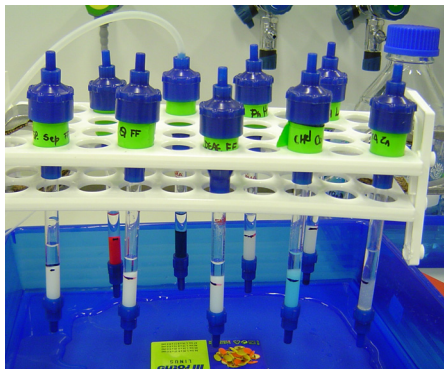

Figure 7: Screening on glass columns.

Several types of strongly basic and weakly basic resins available on the market were evaluated for their capacity to adsorbs carminic acid from the raw extract. Screening experiments were carried out using glass SIGMA liquid chromatography columns (Luer-Lock, Non-jacketed, Size: 1 cm x 15 cm) and 2 g of beaded adsorbent, previously activated and equilibrated. The diverse adsorbents presented particle sizes between 40 and 900 μm in diameter. Matrix base materials included dextran, agarose, styrene- or acrylic-divinylbenzene, silica, or ceramic composites. The functional groups were tertiary, quaternary amines and phenyl groups. 5 ml of aqueous cochineal extract was loaded in each column. Sorption and desorption of the product was carried out batch-wise under gravitational flow. A washing step was performed with equilibration buffer (5 column volumes) and step elution of bound product was promoted by changing the chemical environment. Elution solvents were a) 1 M NaCl in buffer equilibrium; b) 0.1 M phosphate buffer, pH 9; c) same as before containing 5 % isopropanol [34] [35].

3.2.5. Adsorption isotherms

Equilibrium batch adsorption experiments were undertaken in SIGMA liquid chromatography columns (Luer-Lock, Non-jacketed, Size: 1 cm x 15 cm) under gentle mixing conditions (Platform Rocker STR 6, Stuart, UK). 0.10 g of solid support was contacted in each of the columns with 10 ml of buffered solutions with increasing initial dye concentration

(0.38, 0.76, 1.50, 2.30, 3.07, 3.46, 4.00, 5.00 mg·ml^{-1}). The columns were sealed and placed in a shaker at 25°C until equilibrium was reached (18 h). The ion exchanger was then allowed to settle under gravity for approximately 30 min. and the resulting supernatant samples were analyzed using previously described methods [16]. Data was fitted by non-linear regression methods using a commercial software package (GraphPad Prism, San Diego, CA, USA) [36]. The effect of temperatures (4, 25, 55, and 95°C) and ionic strength (0.03, 1.04, 4.55, 8.46 and 15.6 mS·cm^{-1}) on product adsorption at equilibrium was assessed [37].

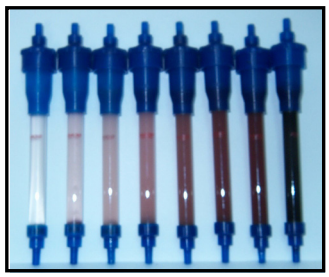

Figure 8: Adsorption isotherm in equilibrium.

3.2.6. Breakthrough curves in packed beds

Complete breakthrough curves were determined from frontal packed bed adsorption experiments in order to evaluate dynamic system performance. A glass column (1.0 cm internal diameter, 10 cm high) mounted vertically was loaded with 4 ml beaded resin. Fluid velocity was 19.1, 76.4, 150, 382.2, or 764.3 cm·h^{-1}. A homemade glass column (2.0 cm internal diameter, 1 m high), mounted vertically, packed with 30 ml adsorbent beads was also employed; fluid velocity was 38.2 cm·h^{-1}. These systems were fed with an

Figure 9: Frontal experiment carminic acid adsorption.

aqueous cochineal extract (C_0 = 0.2-8.0 $kg \cdot m^{-3}$), fractions at the outlet of the column were collected automatically, and the concentration of carminic acid measured as described. For the determination of breakthrough curves, the bed was loaded until the carminic acid concentration in the outlet stream equaled, or was approaching, that of the inlet stream, $\boldsymbol{C_0}$. Equilibrium capacities were determined by integration of the breakthrough curve according [38]. The experimental curve was displayed in terms of dimensionless effluent concentration against the dimensionless throughput parameter [36]. Sorption performance was expressed as the ratio of breakthrough capacity at 10% breakthrough to the equilibrium capacity [39]. Mass transfer coefficients and diffusivities were calculated by minimizing the distance between the experimental breakthrough curves data points and appropriate analytical expressions with the solver add-in function of the Microsoft EXCEL [40] [39].

3.2.7. Adsorption kinetics in finite bath

Batch adsorption experiments were performed in a stirred tank (total volume 0.5 L, 9.0 cm internal diameter, aspect ratio 2:1). A paddle type impeller (4.0 cm diameter) was used for all the experiments. Samples (0.25 ml) were withdrawn at different time intervals for CA determination. The collected data was plotted as normalized concentration as a function of elapsed time. The effect of the stirrer speed was evaluated at 56, 100, 156, and 240 rpm employing a 5% adsorbent load and at 25°C. Adsorbent load was assessed using cochineal extract (0.4 L) contacted with varying amounts of the solid adsorbent (1.6%, 6.6%, and 16.6% adsorbent load) at 25°C. The effect of initial CA concentration was studied at 0.1, 1.0, 2.0, and 9.0 $mg \cdot ml^{-1}$ by contacting the same volume of feedstock with 80 g of

resin. In the later two cases stirrer speed was maintained at 200 rpm and process temperature was 25°C.

3.2.8. Desorption experiments

Screening for efficient desorption of carminic acid from the solid phase was performed in small laboratory columns under gentle stirring and at 25°C. 1.0 g of preloaded material was contacted with 10 ml of various desorption solutions for 3 h. The recovered carminic acid was quantified in the liquid phase and final yields calculated on this basis. Recovery was studied not only as a function of eluent composition but also as a function of eluent volume (2, 5, 10 ml) and number of extraction steps (1, 2, 5 extractions). Kinetics of desorption was performed in a stirred vessel (200 rpm), as described, using 10 g of preloaded resin and 0.1 L of desorbing solution at 25 °C. 0.25 ml samples were taken for carminic acid analysis as in previous studies.

3.2.9. Evaluation of resin reusability

Optimized adsorption-desorption cycles were performed using the same batch of adsorbent in order to evaluate material robustness to repeated use. To this end, small glass columns containing 1.0 g of adsorbent were employed. The solid was contacted with 10 ml of cochineal extract for 1 h under gentle stirring, the exhausted liquid phase was removed, the resin washed and subsequently eluted with acid-ethanol. This cycle was repeated 10 times. Carminic acid total yields (%) were presented as function of cycle number.

3.2.10. Process evaluation at pilot-scale

Pilot-scale evaluation of the adsorption-desorption cycle was performed in a stainless steel tank (0.4 m^3). Mixing was provided by means of mechanical agitation. Typical experiments were carried-out using 5, 10, or 15 kg of adsorbent, which was contacted with optimized cochineal extract (0.15 - 0.30 m^3) at room temperature. The later was prepared employing 10 kg of dried insect bodies in a 0.7 m^3 stainless steel vessel under vigorous stirring, partially clarified by decantation, and pumped into the adsorption-desorption tank. After desorption, the alcoholic carminic acid solution was concentrated by vacuum evaporation up to a final concentration of 5% (w/v). Further product formulation included stabilization by reaction with ammonia under pressure and spray drying. The product from the prototype process was submitted to quality control analysis, including physicochemical, microbiological, and allergenic testing.

4. RESULTS AND DISCUSSION

4.1. Determination of carminic acid

A number of analytical techniques are available for the quantification of carminic acid [41-49]. However, determination of carminic acid is usually performed in industry on the basis of a gravimetric-spectrophotometric technique proposed by the FAO/WHO [5]. This method is not practical and becomes tedious for the evaluation of large amounts of samples e.g., chromatographic fractions. Therefore, a modified version of this procedure was developed. Carminic acid can be measured by direct UV/VIS absorption at 490-500 nm provided that the sample is dilute in a sufficient amount of 0.02 N HCl. This was confirmed by diluting pure carminic acid in acid media and performing a UV/VIS spectral scan (Figure 10); a maximum absorbance peak in the VIS region was detected at 494 nm. Under these conditions the molar absorptive coefficient (ε) for carminic acid is 5800, which allows calculation of carminic acid concentrations using the Lambert and Beer law [32]. Indeed, a linear relationship was found between carminic acid standard solutions (0.00025, 0.00594, 0.00118, 0.00254, 0.00517, 0.01018, 0.01965, 0.03769, 0.06986, and 0.12263 $mg \cdot ml^{-1}$) and VIS absorbance readings at 494 nm ($y = 1.1292\ x$, $R^2 = 0.998$).

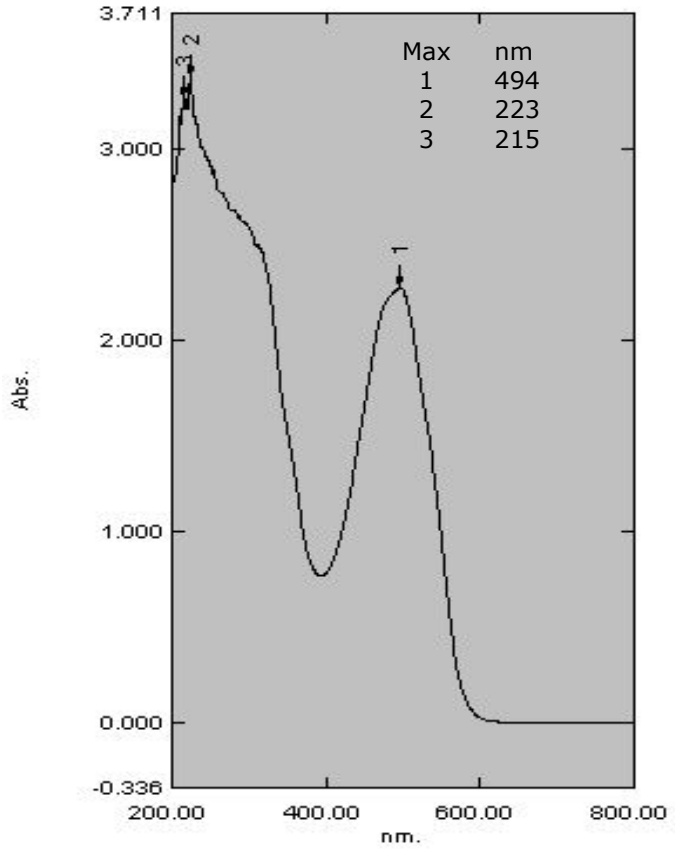

Figure 10: Spectral scan of pure carminic acid in 0.02 M HCl.

The modified VIS method was also statistically compared to the FAO/WHO standard method employing real industrial samples (Figure 11). Both methods were compared employing the Bland-Alman method [50]. The bias value, the average of the difference between both methods was 0.14 and the standard deviation (SD) of bias 3.43 with a 95% confidence interval. These results revealed same discrepancies between the values provided by the two methods with increasing sample concentrations. However, the calculated bias value meant that the two methods had very similar results on average. Therefore, discrepancies found between methods are small enough to render the two techniques as equivalent for routine laboratory work.

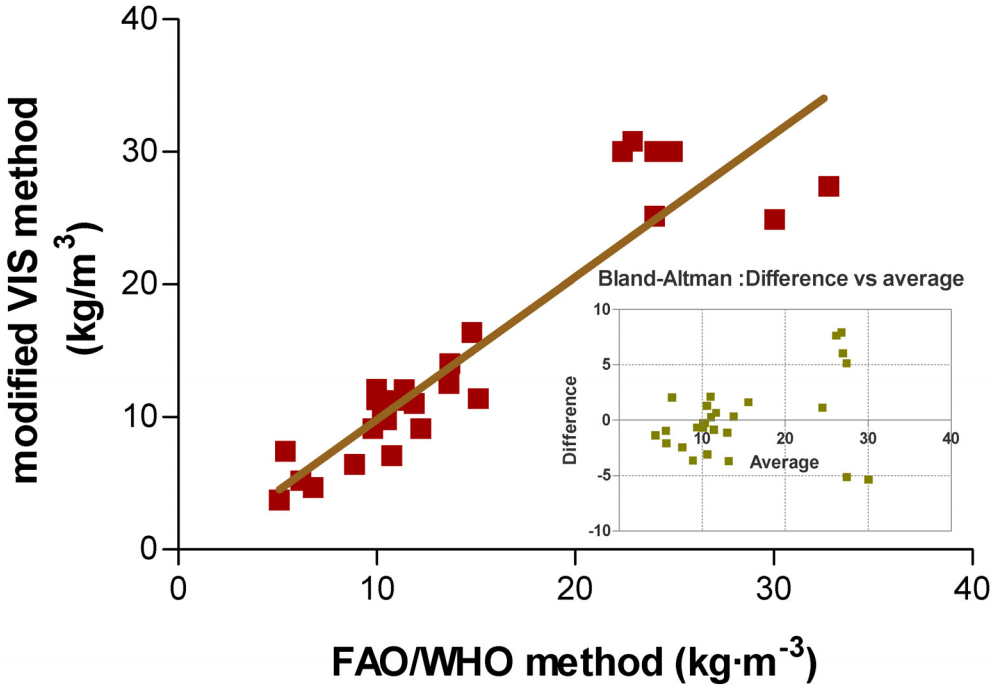

Figure 11: Linear correlation between the modified VIS method and the reference technique for the determination of carminic acid in the concentration range between 0.05 to 1.25 kg·m^{-3}.

The modified spectrophotometric method was additionally compared with a previously published HPLC method [8]. Correlation analysis again showed very good results (y = 0.825 X, R^2 0.999).

4.2. Extraction of carminic acid from cochineal

Naturis S.A. originally implemented an extractive procedure for carminic acid recovery from cochineal on the basis of an alkaline treatment. However, the raw extract produced by this method showed technological drawbacks like sub optimal extraction yields, increased feedstock viscosity, and a tendency to form gels upon cooling. This is probably due to cross-linking between carminic acid and proteinaceous material or other biopolymers present in the sample [51]. Gel formation proved to be problematic at early stages of development due to the high cake resistance encountered during solids removal by plate and frame filtration. This effect was also responsible for increased product losses since the product tended to be trapped within the insoluble fraction. Attempts were made to correct for this effects using intact rather than milled cochineal but overall carminic acid extraction yield suffered from the procedure.

On the basis of these exploratory findings the extraction process was re-optimized and the whole process re-engineered so as to include an adsorption step as the major strategy for product isolation directly from the crude extraction liquor. That means recovery of carminic acid became insensitive to the presence of biological (insect) particulate material. Bartels (1958) [52] showed that the antibiotic streptomycin could be recovered by direct contact of the untreated fermentation broth by contacting with a cation exchange resin. An adsorptive process also would remove most of the potential allergenic proteins presented in the crude extract provided that the appropriate resin and operational conditions are chosen. The use of toxic metallic ions is also prevented.

Several extractive solvents and additives were tested in the search for increased product recovery and for minimized presence of contaminated protein (Figure 12). Extraction with water or diluted buffer solutions, as well as, the presence of the non-ionic detergent Triton X-100 showed moderate extraction. On the other hand, treatment with acid or alkali lead to increased product recovery in the liquid phase. The use of acid is, however, discouraged since it may attack stainless steel surfaces e.g., tank walls and pipes. The main disadvantage in using NaOH for extraction is the concomitant extraction of proteinaceous material. The same was reduced by enzymatic treatment with neutral protease or by further processing employing adsorbent beads with low exclusion limits.

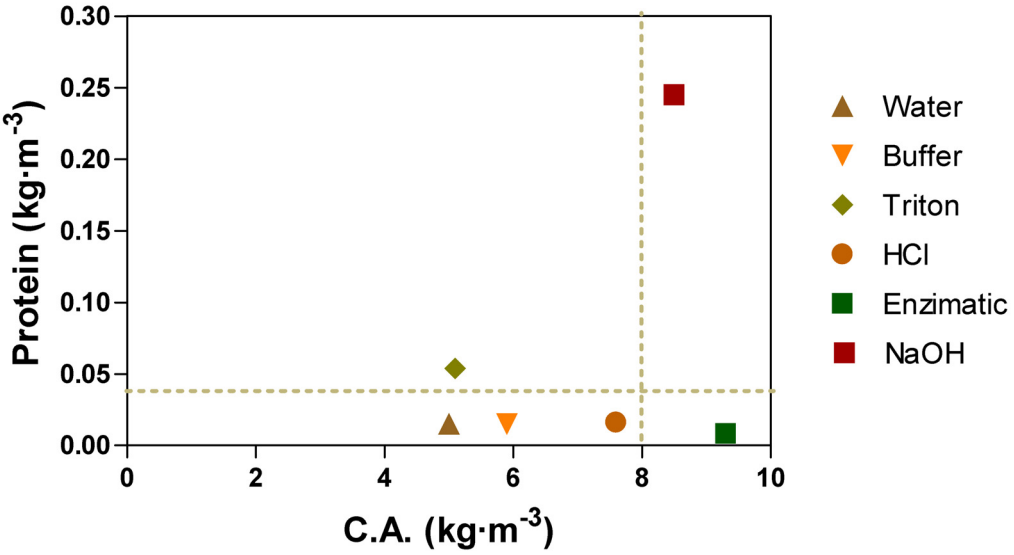

Figure 12: Carminic acid concentrations and total protein levels as a function of the extraction method. The protein level of the extracts were determined according to Bradford [31].

The influence of extraction temperature during extraction was assessed employing a solid (cochineal) to extractant (diluted buffer) ratio 1:20 (Figure 13). Gonzalez (2002) [8] reported that carminic acid is destroyed when exposed to temperatures above 80°C for extended time periods (> 60 min.). On this basis, the extraction experiment was carried out limiting the total extraction time to 30 min. Moreover, extraction efficiency was also found not to increase significantly after 30-45 minutes (data not shown). An extraction temperature of 90°C was chosen as a good compromise between product yield and stability. Figure 13 also depicts carminic acid yields as a function of various solid to liquid ratios. A 1:20 ratio was selected since provided excellent extraction efficiency at moderate dilution rates.

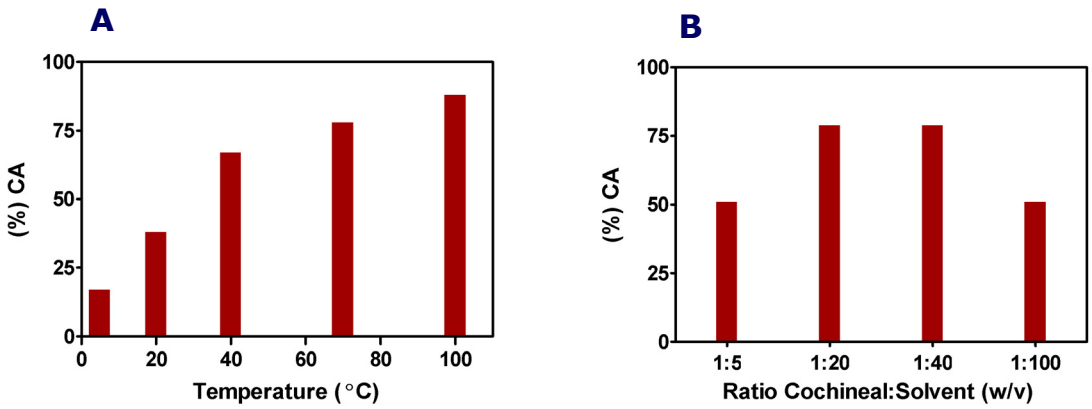

Figure 13: A) The effect of temperature on the extraction of carminic acid. Data is plotted as % of total extracted product in cochineal against extraction temperature (ºC). B) Effect of cochineal-to-solvent ratio on carminic acid extraction efficiency. Ratio is expressed as weight of cochineal to volume of extractant. The carminic acid content of cochineal was 21%.

Extraction studies were performed as a function of the number of extractive steps, using a fixed volume of 50 mM ammonium acetate buffer, pH 6. Figure 14 shows carminic acid yields and the final dilution

rates as a function of the total number of extraction steps. A solid-to-solvent ratio was employed. It can be concluded that more than two extractive steps lead to unacceptable product dilution. Therefore, the final extraction operation was designed in order to find an appropriate balance between total extracted carminic acid and the final dilution rate attained.

These experiments were performed using ammonium acetate buffer due to its increased volatility and availability.

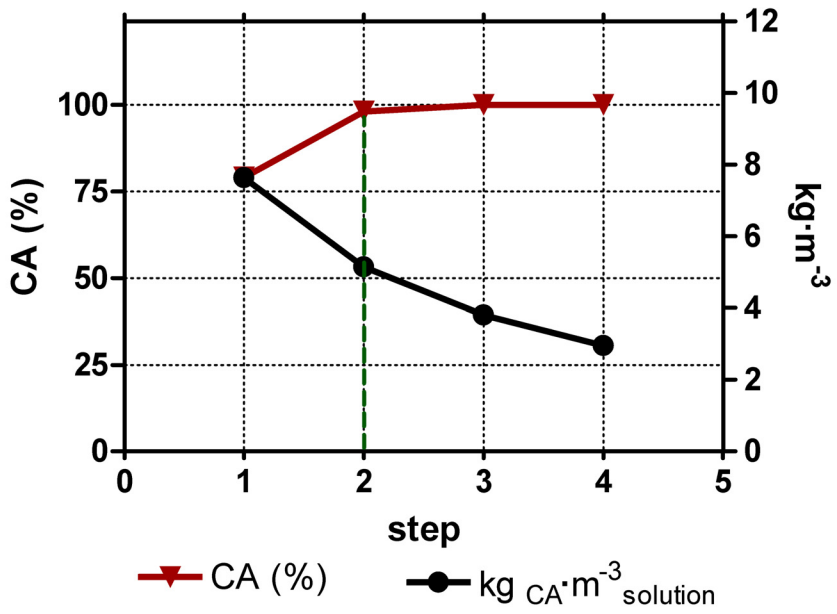

Figure 14: Extraction of carminic acid from cochineal in several steps employing 50 mM buffer ammonium acetate (pH 6) at 90°C during 45 min.

Typical physicochemical properties of the optimized crude extract are summarized in Table 2. These results are compatible with subsequent processing employing adsorption-based unit operations i.e., ion exchange.

PARAMETERS	DATA
Product Concentration	8.7 – 1.0 $kg \cdot m^{-3}$
Protein Concentration	0.21 $kg \cdot m^{-3}$
Density (δ)	1.010 $kg \cdot m^{-3}$ (25ºC)
Viscosity (η)	1.078E-03 $kg \cdot m^{-1} \cdot s^{-1}$
pH	5.1 - 6.2
Conductivity	3.7-5.0 $mS \cdot cm^{-1}$

Table 2: Physicochemical properties of the crude cochineal extract.

4.3. Adsorption of carminic acid on beaded supports

Natural product adsorption on beaded materials is a powerful tool for purification of byproducts at industrial scale. This procedure normally includes the capture of the targeted species from the liquid extract on a solid phase. Later on the product is selectively recovered by modification of the chemical environment provided by the liquid phase e.g., pH, ionic strength, dielectric constant. Selection of the most suitable adsorbent is based on the chemical structural analysis of the product. In the particular case of carminic acid both polar and non-polar interactions with the solid support can be anticipated (Figure 1).

A wide number of solid supports for large-scale adsorption processes are available in the market. These differ in the nature of the base matrix and in the chemical functional groups immobilized on the same. Diverse contacting systems has been described as it is the case of stirred tanks, packed or fluidized beds, and more sophisticated approaches like the spinning basked contactor. In this study, the following aspects has been considered:

- Screening for a suitable adsorbent. This was done by extensive empirical testing employing adsorption-desorption behavior as main selection criteria [53].
- Characterization of carminic acid adsorption behavior at equilibrium onto selected adsorbents (adsorption isotherms).
- Evaluation of adsorption dynamics in packed beds by frontal analysis (breakthrough curves).
- Assessment of adsorption and desorption kinetics in batch stirred vessels (finite bath experiments).
- Estimation of adsorbent reusability regarding process performance and costs.

4.3.1. Screening

In order to identify an appropriate material for the capture of carminic acid from the crude extract, screening experiments were made. A total amount of seventeen solid phases were included e.g., ion-exchangers and hydrophobic interaction adsorbents. Three promising materials were selected as a result of the screening procedure. One of them, Q Ceramic Hyper-D LS (BioSepra SA, Gergy Saint Christophe, France) was discarded at an early stage due to excessive cost for this particular application. A second cheaper group of adsorbents, including 2 (two) materials, was defined. Further studies were oriented towards the use of this second group because of performance, bulk availability, and cost-efficiency. The properties of the chosen ion-exchange adsorbents are summarized in Table 3.

Resin	Type	Matrix	Ligand	Form	Basicity	d_p (μm)
Type-M	Macroreticular	SDVB	TA	FB	Weak	550-750
Type-G	Gel	Polyacrylic	TA	FB	Weak	700-950

SDVB styrene-divinyl benzene; TA: Tertiary amine; FB:Free Base

Table 3: Properties of selected adsorbents.

Beside the selection of the adsorbents showed in Table 4 some interesting observations were made. First, carbohydrate based anion exchangers (Sephadex, Sepharose -Amersham GE Healthcare Biotech, Upsala, Sweden-) displayed high affinity for the product but suffered from a degree of irreversible fouling. On the other hand Phenyl Sepharose, and hydrophobic interaction material, was unable to bind carminic acid even in the presences of 1 M of ammonium sulphate. Finally, same ion-exchange resins strongly capture the product. Attempts to elute the product from these materials using high ionic strength solutions were ineffective. It was later shown that desorption of carminic acid requires a low pH and the presence of an organic modifier in the eluent.

4.3.2. Adsorption equilibrium

The production cost and system/equipment performance, as well as, the mode of operation are major concerns during downstream processing of natural products. Therefore, the system sorption performance in relation to contact time is important to understand process behavior [25]. Both equilibrium and dynamic adsorption characteristics should be studied. Equilibrium data is usually expressed in the form of adsorption isotherms. When the adsorbent is contacted

with the surrounding fluid (feed), product adsorption takes place and, after a sufficiently long period of time, the adsorbent and the liquid phase reach equilibrium. Under such circumstances, the amount of the component (product) adsorbed on the solid phase is related to the remaining product concentration in the fluid phase. Several mathematical expressions are available to account for this phenomenon [54]. Favorable isotherms of the Freundlich or Langmuir type are most commonly used.

Theory

An equilibrium model: In adsorption on ion-exchangers, the adsorbent harboring charged functional groups is balanced by associated counter-ions, whith the target molecule is considered to exist in an ionized state in solution. Upon adsorption to the solid phase, the target molecule displaces the counter-ions. For an ion exchanger equilibrated with monolayer counter-ions, this process can be represented by equilibrium of the form:

$$A + C \underset{k_{-1}}{\overset{k_1}{\leftrightarrows}} AC$$

Where: *A* represents the adsorption site on the ion exchanger, and *C* is the target molecule in solution. Hence, the rate of adsorption is given by:

$$\frac{\partial q}{\partial t} = k_1 \cdot C \cdot (q_m - q) - k_{-1} \cdot q \qquad \textbf{Equation 3}$$

Where: $\boldsymbol{C}$ is the soluble product concentration ($g \cdot dm^{-3}$), $\boldsymbol{k_1}$ and $\boldsymbol{k_{-1}}$ are the adsorption and desorption rate constants respectively, $\boldsymbol{q}$ is the adsorbed product concentration ($g \cdot kg^{-1}$), $\boldsymbol{q_m}$ the maximum capacity of

the adsorbent ($g \cdot kg^{-1}$) and ***t*** represents time (min.) [36]. At equilibrium Equation 3 equates to zero and thus:

$$q^* = \frac{c^* \cdot q_m}{c^* + \frac{k_{-1}}{k_1}} \qquad \textbf{Equation 4}$$

Where: the superscript * denotes values when equilibrium has been reached between the solid and the liquid phase.

Substituting $K_d = k_{-1} / k_1$ in Equation 4:

$$q^* = \frac{c^* \cdot q_m}{c^* + K_d} \qquad \textbf{Equation 5}$$

The relationship between the equilibrium concentration in the solid phase, ($\mathbf{q}^*$), and the equilibrium concentration in the liquid phase, ($\mathbf{C}^*$), at temperature **T**, is called the adsorption isotherm [55]. Equation 5, after Langmuir, is useful in describing the adsorption equilibrium behavior in many biotechnological relevant cases. Langmuir's model of adsorption is applicable to systems where:

(i) adsorbed molecules form no more than a monolayer on the surface thus it is assumed that once a adsorbed molecule occupies a site, no further adsorption can take place at that site;

(ii) each site for adsorption is equivalent in terms of adsorption energy;

(iii) there are no interactions between adjacent adsorbed molecules [29]. Theoretically, the adsorbent has a finite capacity for adsorbate and thus, a saturation value is reached beyond which no further sorption can take place [56].

Other common empirical expression is due to Freundlich, as follows:

$$q^* = K_F \cdot c^{*(1/n)} \qquad \textbf{Equation 6}$$

Where: K_F and n are empirical parameters depending on a particular adsorption system.

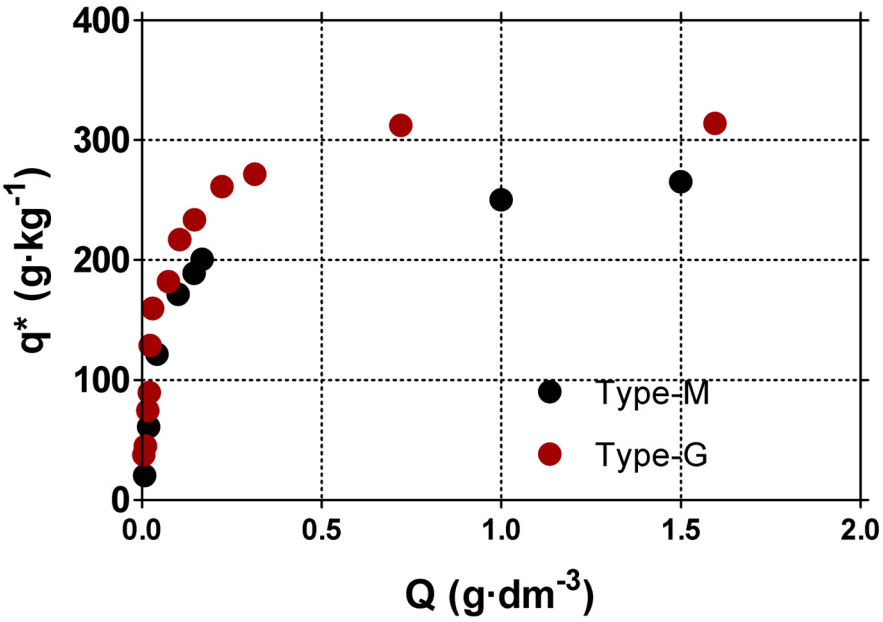

Figure 15: Isotherm of two beaded materials at pH 6, in 50 mM ammonium acetate buffer, at 25ºC. The amount of carminic acid adsorbed per Kg of solid phase is plotted against the remaining carminic acid concentration in the liquid phase at equilibrium.

Experimental equilibrium adsorption data of carminic acid onto the selected adsorbents resin Type-M and resin Type-G is shown in Figure 15. As it was mentioned in the Methods section, experiments were carried out at 25°C and pH 6. Both adsorption isotherms were favorable and obeyed the Langmuir expression as can be seen in Figure 16 [36]. Further, the shape of the isotherms is indicative of a strong dye affinity for the adsorbents. Parameters obtained after non-linear regression analysis are shown in Table 4.

Similar parameter values were found for the two systems under study; maximum capacities ($\boldsymbol{q_m}$) were 250-300 $g \cdot kg^{-1}$ and dissociation constants ($\boldsymbol{K_d}$) were ~ 0.05 $kg \cdot g^{-1}$. These values are in agreement with those found for the adsorption of lactic acid on anion-exchange resins [57, 58]. The Langmuir adsorption isotherm has also been employed to describe many other adsorption systems like proteins on cation-exchanger particles [36], acid dyes on chitin or chitosan materials [56] [59], and organic acid adsorption onto anion-exchange resins [26]. It should be pointed out that adsorption of dyes on solid supports is frequently described by the Redlich-Peterson isotherm due to the existence of stacking phenomena, which is however not present in the carminic acid system. This was demonstrated early by our own measurements of serial standard dilution-absorbance measurements (data not shown).

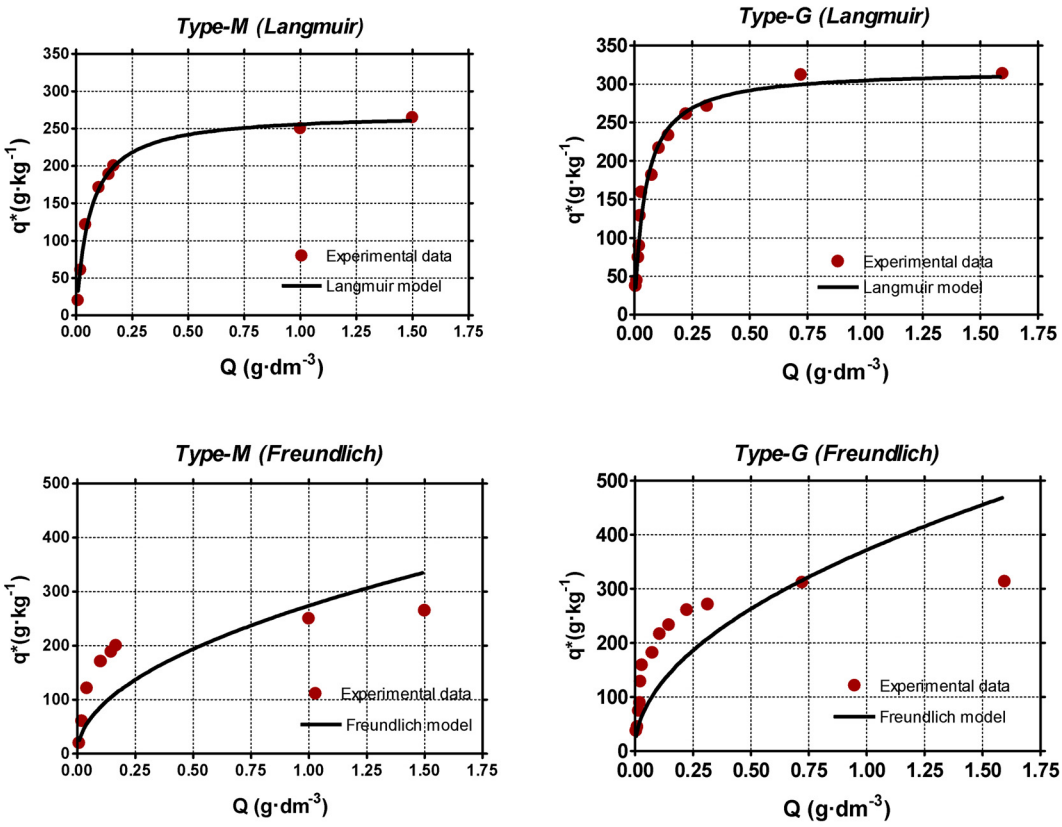

Figure 16: Isotherms for adsorption of CA on Type-G and Type-M materials. The solid lines show fitting of the experimental data to mathematical expressions using non-linear regression analysis.

Resin	Regression Parameters			Statistical Parameters	
	K_d ($kg \cdot g^{-1}$)	95% confidence limit for K_d	q^* ($g \cdot kg^{-1}$)	95% confidence limits for q_o	R^2
Type-M	0.061	0.048 to 0.074	271	256 to 286	0.993
Type-G	0.046	0.035 to 0.057	318	297.6 to 339.9	0.979

Table 4: Parameter values after non-linear regression analysis for the adsorbent systems under study. The Langmuir expression was employed.

Furthermore, carminic acid adsorption on the tested materials followed a Type I isotherm where a definite saturation limit is observed in the absence of adsorbate intermolecular attraction and staking [60].

4.3.3. Effect of temperature and ionic strength

Other variables, namely temperature and ionic strength of the crude liquor, were tested in relation to adsorptive performance. Major differences were not found at different adsorption temperatures within the practical rage of operation (data not shown). On the other hand, solution ionic strength was found to influence the degree of adsorption. From Figure 17 it can be observed that conductivity values > 7 mS·cm $^{-1}$ are deleterious to product capture. This fact limits the addition of salts during the preparation of the cochineal extract.

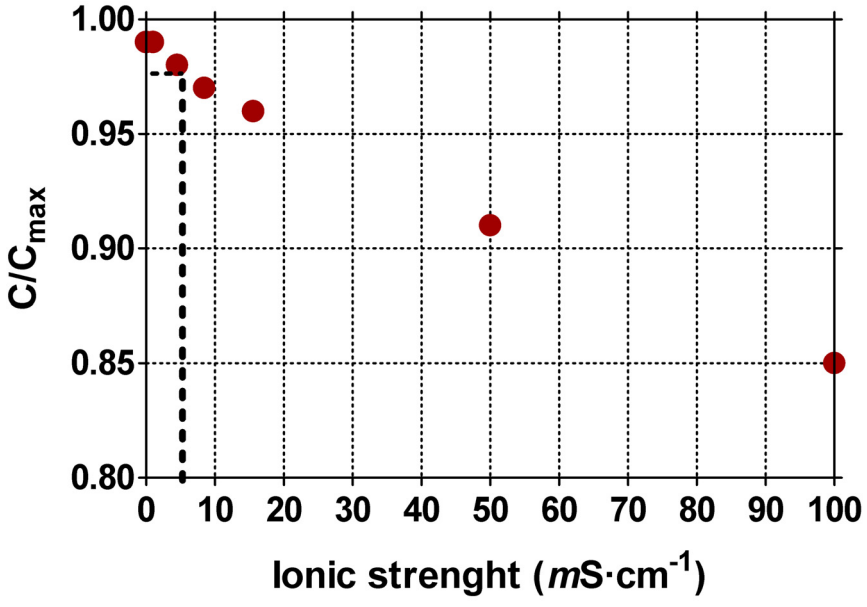

Figure 17: Effect of the ionic strength on the adsorption of carminic acid to the solid support. Fractional maximum adsorption is shown as a function of the process variable conductivity (*m*S·cm^{-1}).

4.3.4. Frontal analysis

The adsorption phenomena onto an anion exchanger are not instantaneous and therefore, mass transfer limitations must also be considered during process characterization.

Theory

The mechanisms of transport: The study of the transport mechanisms make use of mathematical expressions for the velocity of the adsorption at the local level, that is the behavior of one isolated adsorbent particle. For one solute molecule to be adsorbed on the solid particle it should –at first- cross from the bulk of the liquid phase to the surface of the adsorbent. However, diffusion in the bulk is usually not considered a major limitation mechanism [29]. On the contrary, mass transfer resistance is primarily found at the particle level. Several resistances to the solute (mass) transfer limitation can be described, as depicted in Figure 18 (ii and iii):

i. *transfer from the bulk liquid to the liquid boundary layer surrounding the particle (bulk diffusion);*
ii. *diffusion through the relatively stagnant liquid film surrounding the particle (film diffusion);*
iii. *transfer through the liquid in the pores of the particle to internal surfaces (porous adsorbents) or diffusion into the solid (gel type particles), that is intraparticle diffusion;*
iv. *binding at the reaction site.*

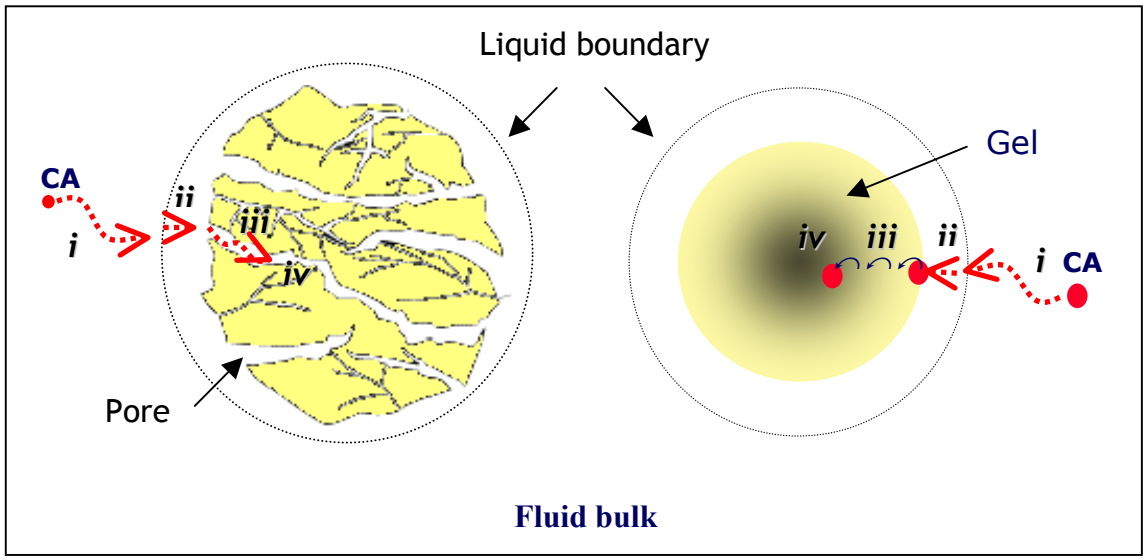

Figure 18: Mass transfer limitation involved in adsorption of a solute from liquid bulk to a porous or gel type adsorbent particle.

The parameters of mass transfer mechanisms are difficult to measure by direct methods; they can however, be estimated by fitting experimental data with appropriate mathematical models. Frontal experiments are useful to understand the adsorptive behavior in packed-beds. Breakthrough curve experiments were performed and analyzed by a classical mathematical **Film and pore diffusion model** for the Type-M beaded material [36],[40]. This model is characterized by external mass transfer limitations and by intraparticle diffusion occurring through the liquid-filled voids (pores) of the adsorbent particles. A solid diffusion model was also applied to data obtained with the Type-G material [55]. Development of analytical expressions to simulate different adsorptions systems implies the following assumptions: a) the adsorbent particles are spherical, with uniform size and density, and the functional groups of the ion exchanger are distributed evenly throughout the interior of the particle; b) the mass transfer from the bulk liquid to the liquid boundary layer surrounding

the particle is negligible; c) mass transfer to the surface of the adsorbent is governed by film diffusion, which is characterized by a mass transfer coefficient (***k_f***); d) the adsorbent is a porous material into which the solute must diffuse. This is characterized by the pore diffusivity (***D_p***); e) surface reaction between the adsorbate and an adsorption site is both irreversible and infinitely fast. Adsorption is isothermal, and its equilibrium behavior can be represented by a rectangular isotherm; f) axial dispersion is negligible in packed bed *systems.*

4.3.4.1. Breakthrough curves on Type-M resin

One of the materials studied, the Type-M adsorbent, has a macroporous nature. Therefore, when it is used in a packed-bed configuration both liquid film AND pore diffusion limitations can be anticipated. For external mass transfer limitations:

$$\dot{N} = k_f \cdot A \cdot \left(C_i - C_i^s\right) \qquad \textbf{Equation 7}$$

Where: ***C_i*** and ***C_i^s*** are the solute concentrations in the bulk fluid and at the particle surface, respectively and A is the surface area of the particle. This mechanism is dominating when product concentration is low in the bulk fluid and the flow regime is laminar. For conventional packed bed adsorption the transport coefficient (***k_f***) describing this mechanism has been correlated with dimensionless numbers as the particle Reynolds number and the Schmidt group. To estimate ***k_f*** in this systems the following correlation can be employed after of Foo and Rice [27, 36, 61]:

$$k_f = \frac{D_{AB}}{d_p}(2 + 1.45 \cdot \mathrm{Re}_p^{1/2} \cdot Sc^{1/3}) \qquad \textbf{Equation 8}$$

were $\boldsymbol{D_{AB}}$ is the molecular diffusivity of carminic acid in free aqueous solution ($m^2 \cdot s^{-1}$), $\boldsymbol{d_p}$ is the mean particle diameter (m), $\boldsymbol{Re_p}$, is the particle Reynolds number (-) and $\boldsymbol{S_c}$, the Schmidt number (-). $\boldsymbol{D_{AB}}$ was estimated using the semi-empirical correlation after Polson [27] from the absolute temperature ***T***, the solution dynamic viscosity η, and the molecular weight of the colorant ***M*** as denoted in Equation 9:

$$D_{AB} = 9.4 \cdot 10^{-15} \frac{T}{\eta \cdot (M)^{1/3}} \qquad \textbf{Equation 9}$$

The particle Reynolds number, which is based on the single particle settling velocity and the particle diameter, is defined as follows:

$$\mathrm{Re}_p = \frac{U \cdot \rho_p \cdot d_p}{\eta} \qquad \textbf{Equation 10}$$

Where: ***U*** is the linear superficial velocity of the liquid flowing through the column ($m \cdot s^{-1}$), and ρ_p is the particle density ($kg \cdot m^{-3}$). The Schmidt group, which relates the momentum transfer to the mass transfer, is defined according to Equation 11:

$$S_c = \frac{\eta}{\rho_l \cdot D_{AB}}$$ **Equation 11**

Where: ρ_l is the liquid density.

In a simple case, and assuming a particle with internal pores of uniform size, the following Equation 12 can be use to estimate the diffusion of the product into the pores (***D_p***) [62]:

$$D_p = D_{AB}\left[\frac{\varepsilon_p}{2-\varepsilon_p}\right]^2$$ **Equation 12**

Where: ε_p is the intraparticle porosity.

Mass transfer parameters were theoretically calculated from correlations and experimentally validated under standard process conditions employing the Type-M resin for carminic acid adsorption using Equation 8 and Equation 12; ***k_f*** value was calculated to be 3.28E-06 $m \cdot s^{-1}$ and ***D_p*** 1.69E-11 $m^2 \cdot s^{-1}$. These values are in agreement with the ones reported for the adsorption of BSA [36] and Lysozyme on S-Sepharose FF and for the adsorption on β-galactosidase on porous silica [63]. Furthermore, frontal experiments performed with the carminic acid / Type-M resin system showed to fit to the film and pore diffusion model according to Hall (Figure 19 and Table 6). Experimentally determined values for the mass transfer parameters were found to be 3.0E-06 $m \cdot s^{-1}$ for ***k_f*** and 4.0E-11 $m^2 \cdot s^{-1}$ for ***D_p***.

Therefore, excellent agreement was found between calculated and experimental values.

In order to evaluate the relative importance of the intraparticle diffusion resistance to film diffusion resistance the Biot number (***Bi***) can be employed:

$$Bi = \frac{k_f \cdot R_P}{D_p} \qquad \textbf{Equation 13}$$

For ***Bi*** << 1, external mass transfer resistance is the controlling mass transfer step, while for ***Bi*** >> 100 pore diffusion is the predominant mass transfer controlling mechanism. Biot numbers between 1 and 100 indicate that both mass transfer mechanisms are involved for the particular process [64]. In our case, the values for calculated vs. experimental Biot numbers were 48 and 18, respectively. Therefore, a combined mass transfer resistance mechanism is confirmed for the adsorption of CA onto the Type-M beaded support.

Some other data can also be derived form the frontal experiments. The experimental breakthrough curve allowed the calculation of both dynamic and equilibrium capacities of the adsorbent for carminic acid. $\boldsymbol{Q_{dyn}}$ obtained from the curve was 16.5 $g \cdot kg^{-1}$ of resin at 10% of breakthrough. This represents 36% of the total available equilibrium capacity (59.3 $g \cdot kg^{-1}$) under the superficial velocity conditions fixed during this experiment.

Column parameters	Type-G resin	Type-M resin
Particle radius (m)	3.5E-04	3.5E-04
Bed length (m)	0.052	0.09
Column int. diameter (m)	0.01	0.02
Initial CA concentration ($kg \cdot m^{-3}$)	7.44	4.5
Void fraction (-)	0.35	0.35
Matrix volume (m^3)	4.08E-06	2.83E-05
Volumetric flow rate ($m^3 \cdot s^{-1}$)	4.16E-09 - 1.7E-07	3.33E-08
Fluid velocity ($cm \cdot h^{-1}$)	19.1 - 764.3	38.19719

Table 5: Characteristics of the packed-bed systems for the experimental determinations of breakthrough curves employing Type-G and Type-M resins.

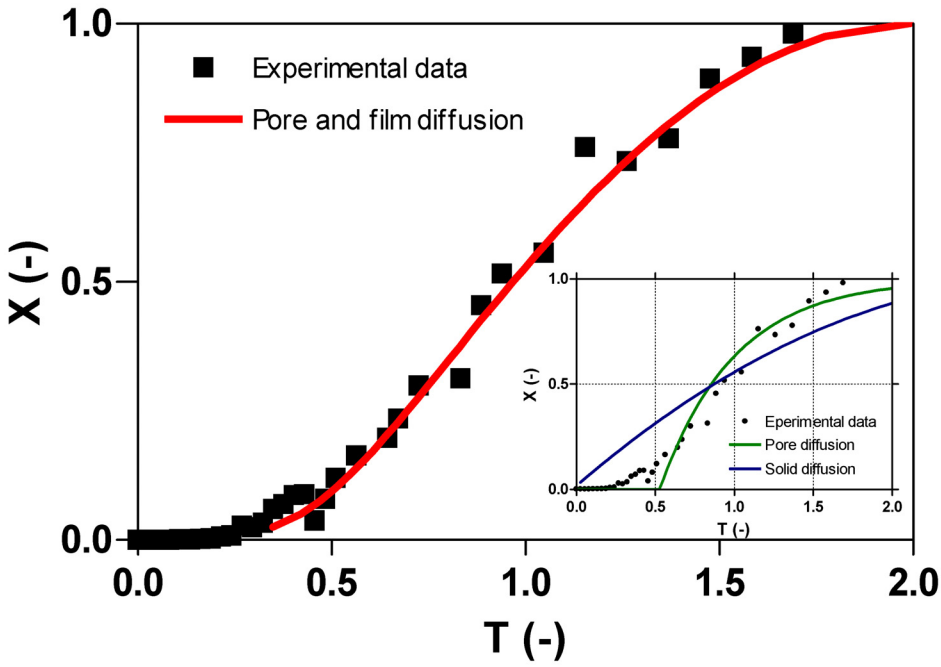

Figure 19: Frontal analysis for the Type-M resin in packed bed. Normalized experimental data were fitted using the pore and film diffusion model after Hall (1966).

$$T = 1 + \left(\frac{1}{N_{pore}} + \frac{1}{N_{film}} \right) \times \left(\frac{\Phi(X) + \frac{N_{pore}}{N_{film}} \times (LN(X+1))}{\frac{N_{pore}}{N_{film}} + 1} \right)$$

Where

$$\Phi(X) = 2.39 - 3.59 \times \sqrt{(1-X)} \qquad T = \frac{C_0 \times u \times t}{Q_{eq} \times L} \qquad X = \frac{C}{C_0}$$

$$N_{film} = \frac{3 \times K_f \times L}{r_p \times u} \qquad N_{pore} = \frac{15 \times D_e \times L \times (1-\varepsilon)}{u \times r_p^2}$$

Table 6: Pore and film diffusion model after Hall (1966). *T* **is the dimensionless throughput.** N_p **and** N_f **are mass transfer numbers.**

4.3.4.2. Breakthrough curve on Type-G resin

The dynamic adsorption behavior of a second solid support, Type-G, was also evaluated frontal load on a packed bed; column dimensions and operational parameters are summarized in Table 5. The very structural nature of this beaded gel creates the frame for solid diffusion mass transfer limitations, as a major contribution to the particle side diffusivity. Figure 20 depicts calculated curves after the non-linear regression analysis of the experimental data using the homogeneous model after Yoshida (1984) [55]. In this case liquid film side mass transfer resistance was neglected for D_s calculations.

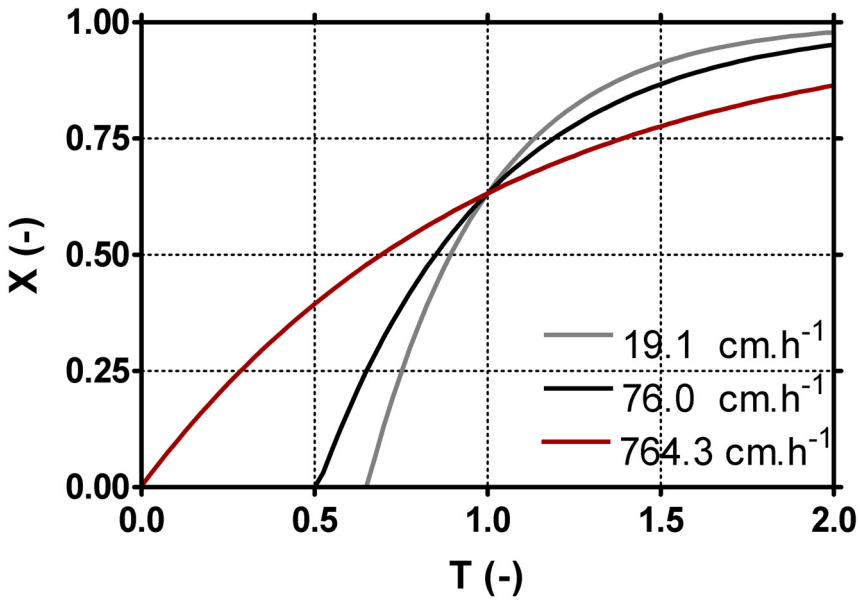

Figure 20: Frontal analysis for the Type-G resin in packed bed. Normalized experimental data were fitted using the homogeneous model after Yoshida (1984). Experiments were performs at different linear flow rates.

Intraparticle diffusion is here supposed to occur by the surface hopping mechanism and the adsorbent is assumed to have a homogeneous

surface with a uniform structure Figure 18. A transfer number N_s accounting for solid diffusion at the particle side is introduced

$$N_s = \frac{15 \cdot (1-\varepsilon) \cdot L}{D_s \cdot d_p^2 \cdot u} \cdot \frac{Q_{\max}}{C_0}$$ **Equation 14**

Where: ε is the void fraction, **L** is the column length (m), D_s is the solid diffusion coefficient ($m^2 \cdot s^{-1}$), d_p is the particle diameter (m), Q_{max} is the equilibrium capacity ($g \cdot kg^{-1}$), and C_0 is the initial concentration ($g \cdot dm^{-3}$).

The best sorption performance was evidenced working at 19.1 $cm \cdot h^{-1}$ linear flow rate. Under such operational conditions, the experimental value for D_s was 5.6E-12 $m^2 \cdot s^{-1}$. The relative contributions both internal and external mass transfer resistances, are expressed employing the dimensionless parameter δ:

$$\delta = \frac{1}{5} \frac{k_f r_p}{D_s} \frac{C_0}{Q_0}$$ **Equation 15**

A calculated value for δ 1.6, using a k_f value estimated after Foo and Rice (3.2E-06 $m \cdot s^{-1}$) evidences a slightly dominance of the intraparticle mass transfer resistance; a value of 1 is usually taken as cut-off. Meshko et al. (2001) [65] have obtained values ≈ 10E-5 $m \cdot s^{-1}$ for K_f and ≈ 10E-14 $m^2 \cdot s^{-1}$ for D_s during batch adsorption of basic dyes on granular activated carbon and natural zeolite. These discrepancies can be explained considering the use of adsorbents with different particle sizes and physical structure, different initial dye concentrations, and different contacting systems.

4.3.4.3. Performance of the packed bed

Mass transfers coefficients were assessed in the packed bed mode. The values for k_f are expected to remain similar for the two types of adsorbents tested since particle sizes are similar for Type-G and Type-M resins. On the other hand, values of D_p have been reported to be one to four orders of magnitude greater than D_s values for several systems [55]. This is in complete agreement with the corresponding experimental diffusivities found for Type-M and Type-G materials. Comparison of D_s values with the previously reported by others is more difficult since D_s are known to vary with both feedstock product concentration and adsorbent load. Ma et al. (1996) [66] found that effective diffusivities, a parameter including ***Ds***, decreases slowly with increasing initial concentrations of the adsorbate when a Langmuir isotherm is considered.

The mass transfer characteristics of the Type-M and Type-G solid supports in the packed-bed mode of operation indicated the need for long residence times in order to efficiently capture the product. This would require low operational flow rates or very long columns. Both solutions were judged inconvenient to attain a larger productivity at the industrial scale.

Figure 21 depicted the poor sorption performance attained under processing conditions that would be desirable at the industrial plant. This breakthrough curves are characterized by very early product loss upon system feeding, thus limiting to unacceptable extent product isolation. Moreover, the low flow rates required for product capture are incompatible with the use of a fluidized bed systems due to inefficient particle fluidization. Some basic calculations indicate that the processing of 10 kg of cochineal would require 120 kg of matrix

(dimensions of the column: h=1.5 m d=0.32 m) and a total processing time of approx. 87 h. This extremely long processing times limits process overall productivity and crates additional drawbacks since the feedstock is susceptible to microbiological attack and has gelling properties. In turn, this would create even more difficulties during application of the extract to the column e.g., viscous fingering and clogging. Filtration is also prevented due to increased cake compressibility (s 0.5-0.8, data not shown) [29].

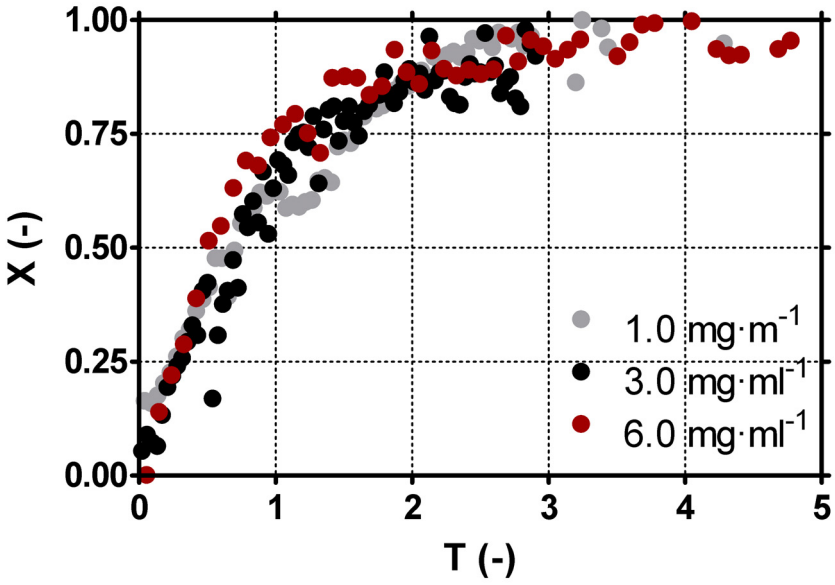

Figure 21: Breakthrough of CA onto Type-G at different initial concentration.

Therefore, an alternative integrative technology for downstream processing of the carminic acid was sough. Technologies, which are able to operate in the presence of particulate biological materials, are recirculation fluidized beds or stirred tanks. Due to the availability of the later at the pilot plant a finite bath adsorption process was selected for further performance studies.

4.3.5. Batch adsorption in finite bath

From the previous section on dynamic adsorbent performance analysis in packed-beds it is known that combined mass transfer mechanisms are present during the adsorption of carminic acid Type-M and Type-G materials. Combined mass transfer resistances has been reported, for example, by Fernandez and Carta (1996) for the adsorption of BSA on composite silica materials and by Atun and Hisarli for the adsorption of carminic acid on glass powder [67, 68].
As an alternative to the use of packed adsorbents, experiments in stirred contactors were performed in order to evaluate a potential reduction in the mass transfer resistances. This would lead to efficient product capture in a simpler operational mode. Moreover, direct batch adsorption can be performed without extensive previous clarification of the feedstock.

Some basic assumptions were made in order to simplify the analysis of the system [30]: a) the porous adsorbent particles are supposed to be suspended in a perfectly mixed tank and the bulk concentration of the adsorbate is taken to be uniform in the liquid phase; b) there is no variation in the total volume of the tank during the process (finite bath); c) external mass transfer resistance exists at the fluid film surrounding each particle; d) the transport of adsorbate within the adsorbent particle (intraparticle diffusion) is also limited; e) the adsorption process is considered to be isothermal. As it was the case for packed beds, single component adsorption is considered to occur. Additionally, the mass transfer from the bulk liquid to the liquid boundary layer surrounding the particle is taken as negligible.

During the adsorption of carminic acid in a finite bath –the batch stirred contactor- the dye concentration in the liquid phase is reduced

from CA_0 to CA_f while the dye concentration on the adsorbent increases from q_o to q_f. The mass balance equation is then written as follows:

$$V \cdot (CA_0 - CA_f) = W \cdot (q_0 - q_f) \qquad \textbf{Equation 16}$$

Where: V is the volume of the liquid phase (L), W is the amount of adsorbent added (kg) and q_o and q_f are the initial and final concentration of carminic acid on the beaded material ($g \cdot kg^{-1}$).

As a first step to understand the influence of major processing parameters on the adsorptive performance of the finite bath, system batch contact-time studies were performed. The influence of the impeller velocity on particle suspension and adsorption kinetics, as well as, the effect of the adsorbent load on process performance was assessed. Initial CA concentration was in the range 8-10 $g \cdot dm^{-3}$ since the optimized extraction protocol and the same cochineal bulk samples were used (Table 2).

4.3.5.1. Mixing and particle suspension

Effect of stirrer velocity

Mixing in the batch contactor was studied at different stirrer speeds, thus creating different flow patterns in the system. The dimensionless parameter used to characterize the fluid flow is the impeller Reynolds number, Re_i. For stirred vessels, Re_i is defined as:

$$\mathrm{Re}_i = \frac{N_i \cdot D_i \cdot \rho_l}{\eta}$$ **Equation 17**

Where: N_i is the rotational speed (s^{-1}), D_i impeller diameter (m), ρ_l fluid density ($kg \cdot m^{-3}$), and η is fluid viscosity ($Pa \cdot s^{-1}$). Values for Re_i characterizes the flow regime in a system to be laminar ($Re_i \leq 10$), transition, or turbulent ($Re_i \geq 10{,}000$). Mixing efficiency also depends on the impeller design and the tank geometry. Stirred tank laboratory experiments were performed at 56, 100, 156, 200, and 240 rpm, as described under Methods. Calculated Re_i were between 2,380 and 10,200 which can be well considered describing the transition to turbulent flow regime in tanks of small dimensions as opposed to industrial ones [29, 69].

The Reynolds group can be related to the required mixing power employing the power number N_p, defined as:

$$N_p = \frac{P}{\rho_l \cdot N_i^3 \cdot D_i^5}$$ **Equation 18**

Where: **P** is power ($kW \cdot m^{-3}$), ***Ni*** is the stirrer speed (s) and D_i is the impeller diameter (m). The relationship between Re_i and N_i depends on the flow regime in the tank. In laminar regime the N_p is inversely proportional to the Re_i whereas at turbulent regime the $\mathbf{N_p}$ is independent to the Re_i [29]. Calculated power consumption per unit volume to attain the corresponding Re_i values was between 1 and 82 ($kW \cdot m^{-3}$). Energy delivered to impellers in stirred contactors is an important consideration in process economics and scale-up.

The stirring speed have had two limiting conditions, that is: a) the stirrer velocity must be enough to suspend the adsorbent particles

and, b) liquid stirring should not promote vortex formation, since this would decrease the friction coefficient between liquid and suspended solid particles. The first condition i.e., appropriate particle suspension was evaluated *via* the Zwietering (1958) criteria [70]. The minimum power input to obtain a complete suspension is defined as a critical stirrer speed (***n_c***). This parameter can be estimated from the following empirical correlation:

$$n_c = \frac{s \cdot d_p^{0.2} \cdot \eta^{0.1} \cdot B^{0.13} \cdot (g \cdot \Delta\rho)^{0.45}}{\rho_l^{0.55} \cdot D^{0.85}} \qquad \textbf{Equation 19}$$

$$s = k \cdot (D_T / D_i)^{\alpha}$$

$$\Delta\rho = \rho_s - \rho_l$$

Where: ***s*** is a constant related to the system geometry (-); ***d_p*** is the main particle diameter (m); η is the dynamic viscosity ($m \cdot s^{-2}$); ***g*** is the gravity acceleration ($m \cdot s^{-1}$); ρ_s is the solid density ($kg \cdot m^{-3}$); ρ_l is the liquid density ($kg \cdot m^{-3}$); ***B*** is the solid concentration % (w/w); ***D_i*** is the impeller diameter (m); and ***D_T*** is the tank diameter (m). ***k*** and α are constants which usually take values 1.5 and 1.4, respectively. Calculated Zwietering parameter for the beaded materials employed in this study was 135 min^{-1}. Moreover, preliminary testing on particle suspension was carried out in buffered aqueous media to evaluate actual resin suspension as a function of the stirrer speed. It was observed (Figure 22) an excellent correlation between experimental and estimated power inputs for complete particle suspension in the vessel.

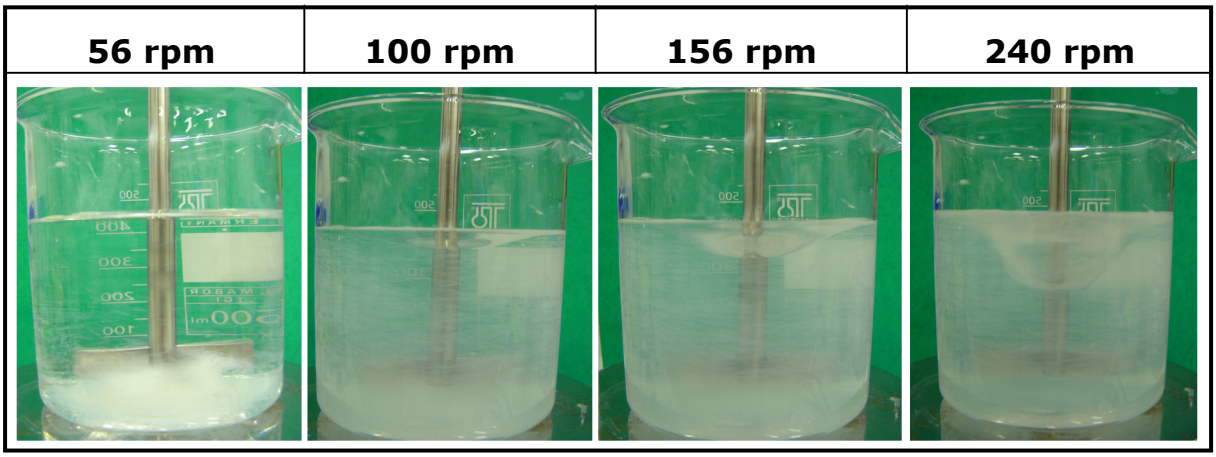

Figure 22: Effect of the stirrer speed on particle suspension

4.3.5.2. Product adsorption.

Adsorption Kinetics. Influence of stirrer velocity and adsorbent type

Once that appropriate condition for liquid and solids contacting were provided, kinetic studies were performed. The mass transfer resistances limit the uptake of carminic acid from the liquid phase to the beaded adsorbent. These resistances can be influenced by the flow regime in the stirred vessel. For example, it is known that the resistance to diffusion across the liquid film around the particle is minimized in the turbulent regime [29]. Therefore, power input can also influence product adsorption in stirred contactors. Figure 23 depicts the influence of stirrer speed on carminic acid uptake from a crude extract on Type-M and Type-G resins as a function of process time. Normalized concentrations are employed for data representation.

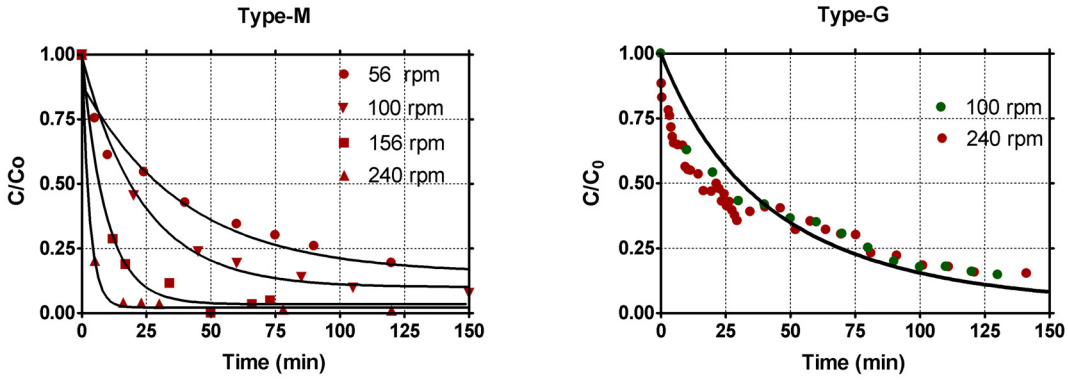

Figure 23: Adsorption kinetics of carminic acid on Type-M and Type-G materials at various stirring speeds. Points represent the experimental data and solid lines show fitting of the experimental data to mathematical expressions (Equation 20) using non-linear regression analysis.

Time course uptake experiments were analyzed employing an empirical kinetic rate constant model [36]. This is based on a *lumped* adsorption rate constant as a single adjustable parameter. The model assumes that the entire rate limiting mechanisms can be represented by this kinetic rate constant (***k₁***), according to Equation 20:

$$C = C_0 - \frac{v}{V}\left[\frac{(b+a)\left(1-\exp\left\{-\left(\frac{2\cdot a\cdot w}{V}k_1\cdot t\right)\right\}\right)}{\frac{(b+a)}{(b-a)}\left(1-\exp\left\{-\left(\frac{2\cdot a\cdot w}{V}k_1\cdot t\right)\right\}\right)}\right] \qquad \textbf{Equation 20}$$

Where:

$$a^2 = b^2 - \left(\frac{C_0\cdot V}{w}\right)\cdot q_m$$

$$b = \frac{1}{2}\left(\frac{C_0\cdot V}{w} + q_m + \frac{K_d\cdot V}{w}\right)$$

and C_0 is the initial liquid phase concentration ($mg \cdot ml^{-1}$), w is the mass of ion exchanger present (mg), V the volume of liquid external to the ion exchanger and q_m an K_d are the Langmuir parameters. A similar approach was successfully undertaken by other authors for systems of industrial relevance like the recovery of lactic acid or proteins from fermentation broth [36, 57, 71]. Values for the lumped kinetic constant were calculated for the adsorption of carminic acid on Type-M (Table 7) and Type-G materials.

Stirrer speed (s^{-1})	Re_i (-)	$K_1 \cdot 10^{-2}$ ($ml \cdot mg^{-1} \cdot s^{-1}$)
0.9	2.38E+03	0.147
1.7	4.24E+03	0.158
2.6	6.63E+03	0.748
4	1.02E+04	2.435

Table 7: Estimated lumped kinetic constant for the adsorption of carminic acid on Type-M resin as a function of stirrer speed in finite bath. R^2 was typically ≥ 0.995.

These data showed two distinct adsorption kinetic behavior patterns, depending on the material utilized. Adsorption kinetics of carminic acid by the Type-G resin remains unaffected as a function of stirrer velocity. Kinetic constant value was found to be 0.251 ± 0.03 E-02 $ml \cdot mg^{-1} \cdot s^{-1}$. This is a classical behavior observed in most adsorption systems that are composed of organics and suspended small particles [67]. On the other hand, when adsorption was performed on the Type-M solid support faster kinetics was

observed upon increasing the power input to the tank. On the basis of these results, and recalling that the kinetic constant is related to the global mass transfer in the system, the later must steadily decreased with increasing stirring speeds. This behavior is completely unusual and will be further discussed in the following sections. The practical implications of this particular finding are dramatic since allowed a 17 times increment in the kinetic constant, from the originally sorption performance to the maximum allowable under actual operational conditions (Table 7). These results cannot be explained solely base on the assumption of a reduce film mass transport resistance.

Adsorption Kinetics. Influence of resin load

Equation 20 can be employed to predict the effect of solids load on the adsorption time profile in the stirred tank. As a first step, the "operating line" for the batch contactor allow for the estimation of the amount of adsorbent required for efficient product capture. This can be done on the basis of the known isotherm (Equation 5) for the materials under study and mass balance system constraints (Equation 16). The graphical solution is presented in Figure 24, from where it can be realized that the rectangular isotherm condition actually holds. This preliminary calculation showed that the ratio amount-of-adsorbent-material-to-liquid-phase-volume for the adsorption of 90 - 99 % of the initial carminic acid present is between 2.9 – 4.7 %. This percentage refers to the adsorbent mass required per feedstock volume to be treated. These conclusions are valid for the two materials under study since their respective isotherms parameters are with a close range.

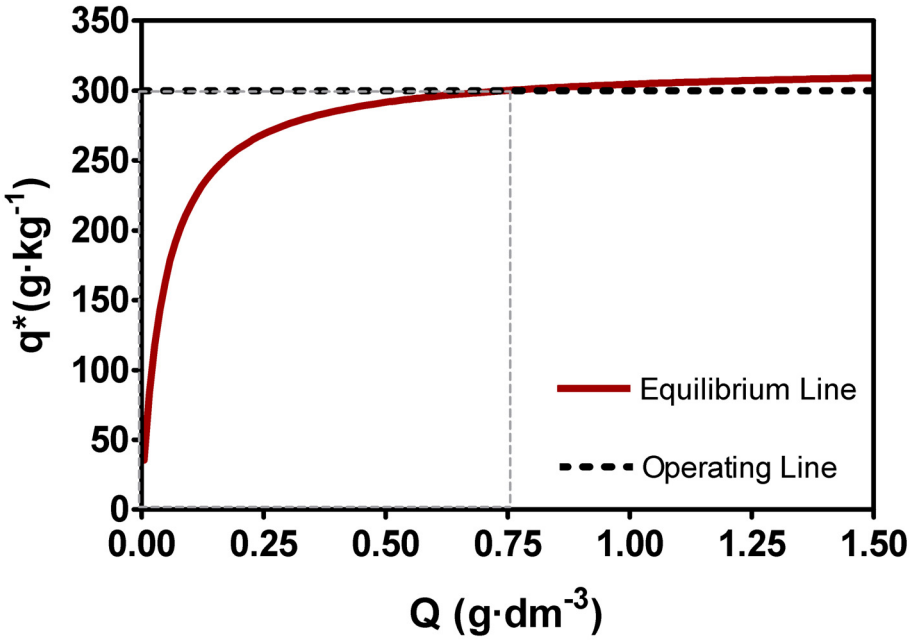

Figure 24: Operating line for 90% recovery of CA onto Type-G in finite bath. Solid line is the isotherm at pH 6, in 50 mM ammonium acetate buffer, at 25°C.

On the basis of the previous estimate provided by the operating line, it was decided to experimentally test the effect of adsorbent load at three different ratios. These experimental values were compared with a theoretical estimation according to Chase (1990). The effect of the adsorbent mass on the adsorption rate is shown in Figure 25. The ratios mass adsorbent: batch volume was 1.6, 6.6 and 16.6% ($w \cdot v^{-1}$), respectively. A very reasonable agreement was found between experimental data and predicted values. The adsorbed fraction was found to increase while increasing the amount of resin in the system. This behavior is in agreement with the findings of other authors for weak base resins in stirring tanks [57, 68]. These data shows an improved overall uptake kinetics with increasing solid load. This can be explained in terms of an increased offer of available binding sites or reactive surface in the system.

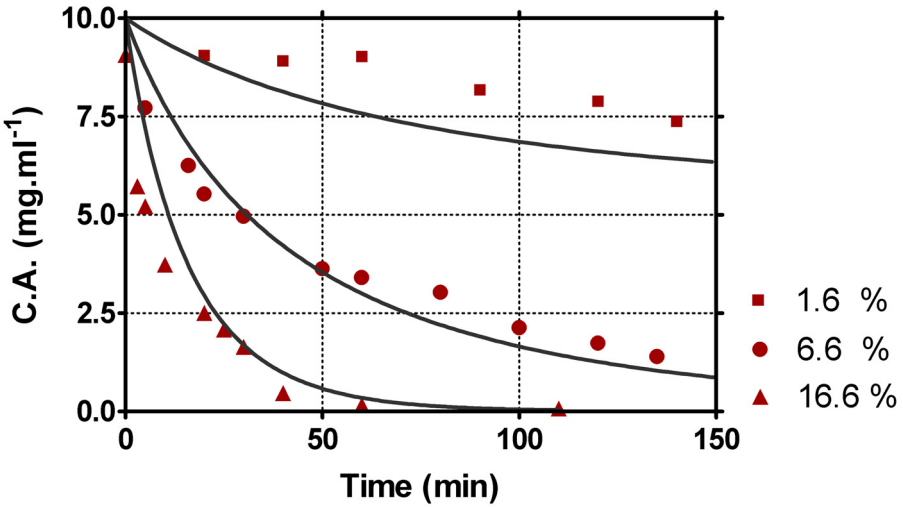

Figure 25: Effect of the adsorbent mass on the carminic acid uptake rate in a stirred tank. The points represent the experimental data (t=25°C, 150 rpm). Solid lines after simulation with Equation 20.

Adsorption kinetics. Influence of feedstock concentration

The influence of carminic acid in the optimized cochineal extract was found to be relatively constant in the range of 8-10 $mg \cdot ml^{-1}$. Therefore, an exhaustive analysis of this parameter on adsorption kinetics was not completely relevant from an operational point of view. In spite of this some kinetic experiments were performed varying the initial concentration (C_0) of colorant in the liquid phase. These studies showed a variation in the calculated values for the kinetic constant (k_1). This dependence of the mass transfer resistances operating in the system and initial product concentration are vastly reported in the literature [67]. In fact, studying carminic acid kinetics as a function of initial concentrations in the liquid phase proved to be an excellent tool to access underlying mass transfer mechanisms during this work.

4.3.5.3. Evaluation of mass transfer resistances

As previously described two major limitations can be present in the system under study, namely external fluid side and particle side mass transfer resistance mechanisms. The observed differences in adsorption kinetics upon varying operational parameters like the stirrer velocity, the adsorbent type, and the solid load could be explained on the basis of these underlying phenomena. Both external and internal mass transfer mechanisms can be present depending on the experimental conditions defined for the system. Moreover, a dominating resistance can prevail or a combination of these two resistance types can coexist.

External mass transfer limitations

External mass transfer occurs across the boundary liquid film layer surrounding the adsorbent particle (Figure 18). This is accounted for by a mass transfer coefficient (k_f) which depends on liquid density, viscosity, temperature, adsorbent particle size and the flow regime [59]. For stirred tanks, k_f can be estimated from theoretical correlations according to Ranz and Marshall [72]:

$$k_f = \frac{D_{AB}}{d_p} \cdot \left(2 + 0.6 \cdot \sqrt{\mathrm{Re}_i} \cdot \sqrt[3]{Sc}\right) \qquad \textbf{Equation 21}$$

$$Sc = \frac{\upsilon}{D_{AB}}$$

Where: Re_i is the impeller Reynolds number (-), **Sc** is the Schmidt number (-), and υ is the kinematic viscosity ($m^2 \cdot s^{-3}$), D_{AB} is the molecular diffusivity of CA in free aqueous solution ($m^2 \cdot s^{-1}$) and d_p is the mean particle diameter (m).

The external mass transfer coefficient can also be determined experimentally. In a finite bath, mass balance boundary conditions can be described by differential equations taking the following assumptions [73] [74]: a) the resin particles are spherical; b) the diffusion of CA in the solid particles follows Fick's law; c) the diffusion process is in the radial direction only and; d) the adsorption takes place under isothermal conditions. The adsorption process can then be described as follow:

For the particles:

$$\frac{\partial q}{\partial t} = \frac{D_s}{r^2}\frac{\partial}{\partial r}\left(r^2 \frac{\partial q}{\partial r}\right) \qquad \textbf{Equation 22}$$

$$r = 0, \quad \frac{\partial q}{\partial r} = 0$$

$$r = R_p, \quad Ds\frac{\partial q}{\partial r} = k_f\left(C - C_i\right)$$

$$t = 0, \quad q = 0$$

and for the liquid film

$$\frac{\partial C}{\partial t} = -\frac{3 \cdot K_f}{R_p}\frac{V_M}{V}\left(C - C_i\right) = -\frac{V_M}{V}\frac{\partial q}{\partial t} \qquad \textbf{Equation 23}$$

$$t = 0, \quad C = C_0$$

When adsorbate concentrations are very low (C_0 ~0) Equation 24 can be integrated yielding the following expression:

$$q = \frac{V \cdot C_0}{V_M}\left[1 - \exp\left(-\frac{3 \cdot Kf \cdot V_M}{R_p \cdot V} \cdot t\right)\right] \qquad \textbf{Equation 24}$$

Therefore, k_f can be experimentally accessed working under experimental conditions leading to the asymptotic case where external mass transfer is dominating [67]. Using this approach, the external mass transfer coefficient was determined by fitting experimental kinetic data obtained at sufficiently low carminic acid concentrations (0.1 $mg \cdot ml^{-1}$) to the preceding equation. Since no effect of stirrer speed on uptake behavior was observed for Type-G material, the same was chosen for k_f determination. Moreover, k_f is know to depend on particle diameter and thus, values experimentally calculated using Type-G resin can be assumed to be equivalent for the Type-M material. This is due to a very similar bead size in both adsorbents. Complete mixing and particle suspension was assured in all these experiments but when working at 56 rpm. Figure 26 depicts the relationship between experimental values for k_f and the stirrer velocity. The external mass transfer coefficient was constant provided that solid were fully suspended e.g., when stirrer speed is higher than the Zwietering criteria. On the other hand, incomplete resin suspension at 56 rpm translated into an enhanced external mass transfer resistance. This can be explained considering that mass transfer between suspended particles and liquid is governed by the energy dissipated around the particles [75]. Moreover, an increase in the mass transfer coefficient can be correlated with the energy dissipation in the fluid phase (ε) since the thickness of the concentration boundary layer, which develops around the particle surface, is considered to

correspond to the size of smallest eddy turbulent field [55] [29] [73]. At steady state, the rate of energy dissipation by turbulence is equal to the power supplied by the impeller and the greater the power input to the fluid, smaller are the eddies.

Comparisons between theoretically derived and experimentally determined values for the external mass transfer coefficient were made (Table 8). The two approaches showed a similar tendency as a function of Re_i although absolute values differed in one order of magnitude. This can be explained on the basis of the influence that suspended biological materials, which are present in the crude extract, might have on the product uptake. Fernandez-Lahore and Thömmes (1999) have described a similar effect during the adsorption of fusion recombinant proteins employing expanded bed adsorption [39].

Summarizing, external mass transfer was held constant at a minimum by stirring at velocities higher than 100 rpm and thus, avoiding the need for implementation of more sophisticated contactor devices like baffled or special tanks [55], spinning-basket contactors [29] or recirculation shallow or fluidized beds systems.

Stirrer speed (min^{-1})	Re_i (-)	k_f experimental ($m \cdot s^{-1}$)	k_f correlation ($m \cdot s^{-1}$)
56	2.38E+03	1.71E-05	1.54E-04
100	4.24E+03	2.62E-05	2.05E-04
156	6.62E+03	2.60E-05	2.56E-04
200	8.49E+03	2.67E-05	2.90E-04
240	1.02E+04	2.76E-05	3.18E-04

Table 8: Experimental and calculated *Kf* as a function of Re_i.

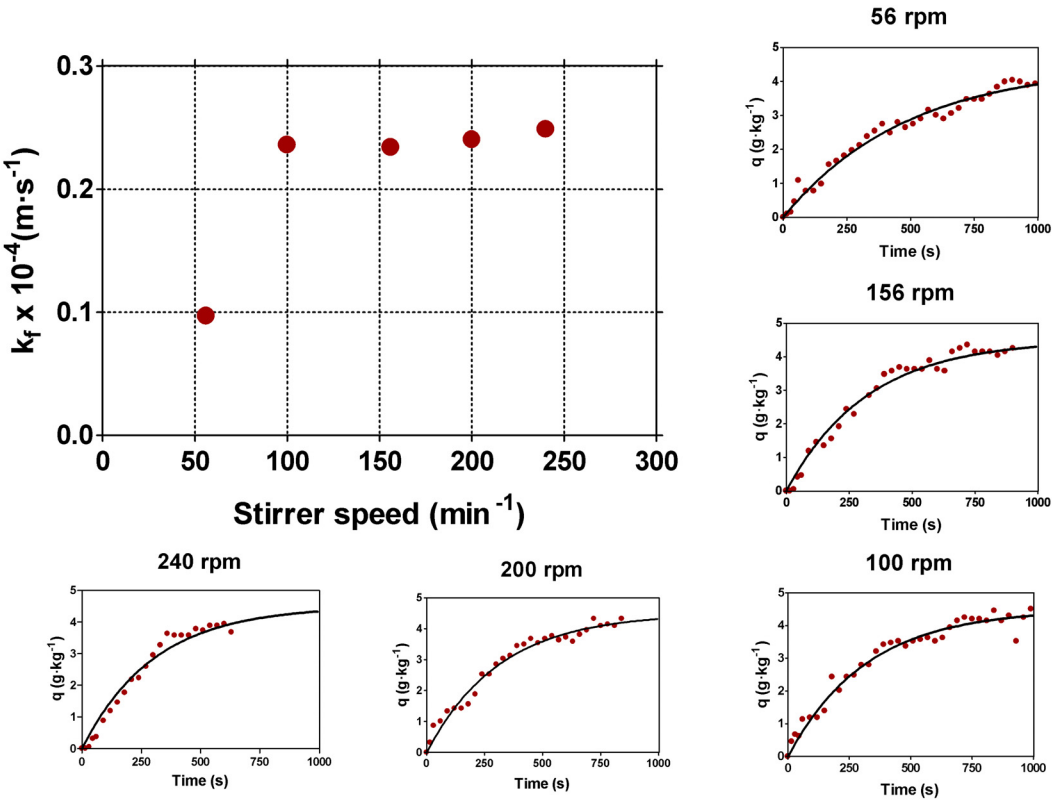

Figure 26: Plot of external mass transfer coefficient (k_f) values obtained experimentally from kinetic profiles at different stirring speeds (56, 100, 156, 200 and 240 rpm) employing Type-G resin. Solid lines are produced after non-linear regression of the experimental data with Equation 25.

Internal mass transfer resistance

Since completely different kinetic profiles were early observed as a function of the resin type (Figure 23), both Type-G and Type-M materials were employed to evaluate experimental intraparticle diffusivities (***D***). This was necessary due to the distinct supposed underlying resistance mechanisms for both beaded supports i.e., solid diffusion and porous diffusion, respectively. Employing a similar principle as the one applied for k_f determination in the previous

section, diffusion coefficients can be determined in the asymptotic case when the initial concentration of carminic acid is very high (C_0~ 9.0 mg·ml^{-1}).

a) Solid diffusivity

The Type-G resin has a gel structure and therefore the assumption of a solid diffusion limiting mass transfer mechanism can be made. This assumption is supported by the fact that frontal packed bed experiments were conveniently fitted employing the homogeneous model. Solid diffusive resistance is accounted by a solid diffusivity (D_s).

Under intraparticle mass transfer control, $q_i=q\ (r_p)\sim q_0$, and Equation 22 can be integrated directly in the following equation:

$$\frac{q}{q_0} = 1 - \frac{6}{\pi^2}\sum_{k=1}^{\infty}\frac{1}{k^2}\exp\left(-\frac{k^2\cdot\pi^2\cdot D_s\cdot t}{R_p^2}\right) \qquad \textbf{Equation 25}$$

For an stirred contactor a useful approximation was given by Helfferich and Plesset [76]:

$$\frac{q}{q^*} \cong \sqrt{1-\exp\left\{\pi^2\cdot\left[-\frac{D_s\cdot t}{R_p^2}+0.96\cdot\left(\frac{D_s\cdot t}{R_p^2}\right)^2-2.92\cdot\left(\frac{D_s\cdot t}{R_p^2}\right)^3\right]\right\}} \qquad \textbf{Equation 26}$$

Where: q is the concentration of carminic acid on the beaded material (g·kg^{-1}); D_s is the solid diffusion coefficient (m^2·s^{-1}); t is the time (min.) and R_p is the particle radio (m).

This expression allow for $\boldsymbol{D_s}$ value determination, as a single adjustable parameter, on the basis of fitting experimental kinetic data by non-linear regression. As was previously stated there is no effect of stirrer speed on time dependent carminic acid uptake by the gel material. Therefore, these experiments were performed in the turbulent regime at stirrer velocities exceeding the Zwietering criteria (200 rpm) for appropriate liquid and solids mixing. This also implies that external mass transfer resistance is reduced to a minimum. Figure 27 depicts experimental kinetic data fitted with Equation 26. Homogeneous diffusivity was calculated to be 3.16E-10 $m^2 \cdot s^{-1}$ (Table 9). This parameter is supposed to be constant at the dye concentrations employed in this study, which corresponds to the rectangular isotherm assumption [64] [65].

Diffusivities for organic acids (citric acid, lactic acid) have been previously reported [26]. These studies were performed in packed beds employing commercial ion exchangers. The diffusivity of lactic acid (MW=96 $g \cdot mol^{-1}$) on a weak anion exchange gel type material, was calculated in the same order of magnitude of that found in this study for carminic acid. Although the diffusion coefficient was calculated on the basis of a pore diffusion component due to the material structure solid diffusion is more likely to predominate. On the contrary, McKay (1998) has reported solid diffusivities ~ 10 E-12 – 10E-13 $m^2 \cdot s^{-1}$ for the batch adsorption of Acid Blue 25 (Bayer), Acid Red 114 (Ciba-Geigy), Basic Red 22 (Ciba-Geigy), and Basic Blue 69 (Bayer) on bagasse pith. Since a number of factors are known to influence diffusion coefficients, this apparent discrepancy can be explained in terms of the different structural nature of the adsorbent employed.

The relative contribution of both external and internal mass transfer resistances was assessed via calculation of the δ factor. This calculation gave a value ~ 0.21 for intensively mixed systems (> 100 rpm) but somewhat lower values at 56 rpm Figure 30. This confirmed a combined mass transfer mechanisms with a lightly dominance on the external component. Under such experimental conditions it can be assumed that the maximum adsorption performance of the matrix was attained. δ factor values for other dye-adsorbent systems e.g., BR22 on pith was 2.5 showing in this case a larger contribution of the particle side limitation. Overall, dye-adsorbent systems seem to develop balanced mass transfer resistances when solid diffusion is the internal limitation ($\delta \sim 1$).

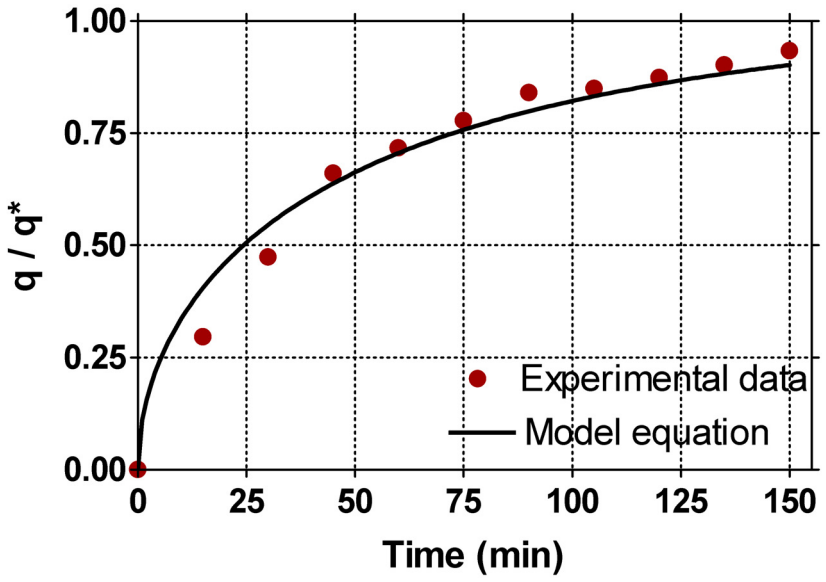

Figure 27: Kinetic adsorption of carminic acid onto Type-G with initial concentration 9.0 mg·ml.

b) Modified porous diffusivity

The Type-M resin has a macroporous structure and therefore the assumption of a porous diffusion limiting mass transfer mechanism can be made. This resistance is usually accounted by the pore diffusivity ($\boldsymbol{D_p}$). Kinetic experiments were performed at high concentrations of carminic acid in the liquid phase, as described in the preceding section, but varying the stirrer velocity (Figure 28). This data were analyzed by non-linear regression, taken ***D*** as a single adjustable parameter, with the following equation [77]:

$$\frac{C}{C_0} = \left(1 - \exp\left(-4 \cdot D_p \cdot \pi^2 \cdot \frac{t}{d_p{}^2}\right)\right)^{1/2} \qquad \textbf{Equation 27}$$

Where: ***C*** is the liquid phase concentration ($g \cdot dm^{-3}$), ***D*** is the diffusion coefficient, ***t*** is the time (min.) and $\boldsymbol{d_p}$ the particle diameter (m).

Figure 28 shows the influence observed between diffusivity values and stirrer velocity. Although it is known that pore diffusivities are not a function of power inputs, nevertheless, these data clearly correlates to the previously calculated lumped kinetic constants (Figure 23). For example the semi-empirical correlation after Polson (1950) can be employed for as a first approximation for $\boldsymbol{D_p}$ values, if corrected for particle porosity (Equation 9 and Equation 12). This correlation shows a major dependence of $\boldsymbol{D_p}$ on the molecular weight of the adsorbent (Table 9). For carminic acid $\boldsymbol{D_p}$ was calculated to be 1.69 E-11 $m^2 \cdot s^{-1}$. Therefore, a modified *augmented* pore mass transfer coefficient must be defined in order to account for the experimental results. Adsorption of carminic acid on Type-M support can be then described in terms of

the modified pore diffusivity (***D*pm**) or *hyperdiffusivity*. This ***D*pm** can be expressed using the following relationship that is able to describe the effect of stirring on the internal mass transfer properties of the adsorbent:

$$D_{pm} = D_p \exp\left(a \cdot \mathrm{Re}_i\right) \qquad \textbf{Equation 28}$$

Where: ***a*** is a constant equal to 5.426E-04. This equation is valid for 2,000 < Rei < 10,000. At lower ***Re*i** numbers (< 2,000) ***D*pm** takes the value of the standard pore diffusivity ***D*p**.

The dependence found between the particle side diffusivity for the porous adsorbent and the flow pattern in the vessel can be explained considering the existence of convective vs. diffusive pores in the structure of the adsorbent beads. In other words a two-mode pore distribution can be assumed. These types of adsorbent particles present a conventional internal porosity distribution but in addition they also present some larger pores, which go through the entire particle. It can be hypothesized that under low stirrer speeds only diffusion occurs into the porous matrix and thus a "classical" pore diffusion limitation is present for the product molecules to reach their reaction (binding) sites. On the other hand, convective flow might be possible when vigorous mixing is provided to the system and turbulence is raised in the liquid phase. Since solid mixing is also expected to increase under such circumstances, slip velocities are concomitantly high. This high liquid to solid relative velocity is known to enhance mass transfer between the phases and can promote convective flow within the macropores. Shorter diffusion pathways in the narrower pores are then available for the product to bind to the reactive sites within the matrix. This behavior is known for certain new generation protein adsorbents (POROS®). This complex porous

structure was also described earlier by Kirkland (1976) [78] and contribution of convective mechanisms -in addition to conventional diffusion- was reported for large size silica particles (Van Kreveld and Van den Hoed, 1978) [79]. These observations can now be extended for the Type-M resin. Frey et al. (1993) [80] has demonstrated the advantages of employing bimodal gigaporous particles for the concentration and isolation of proteins from solutions with moderate efficiency but increased recovery yields [62]. This opens the pave for efficient albeit cheap high-performance processing of natural products.

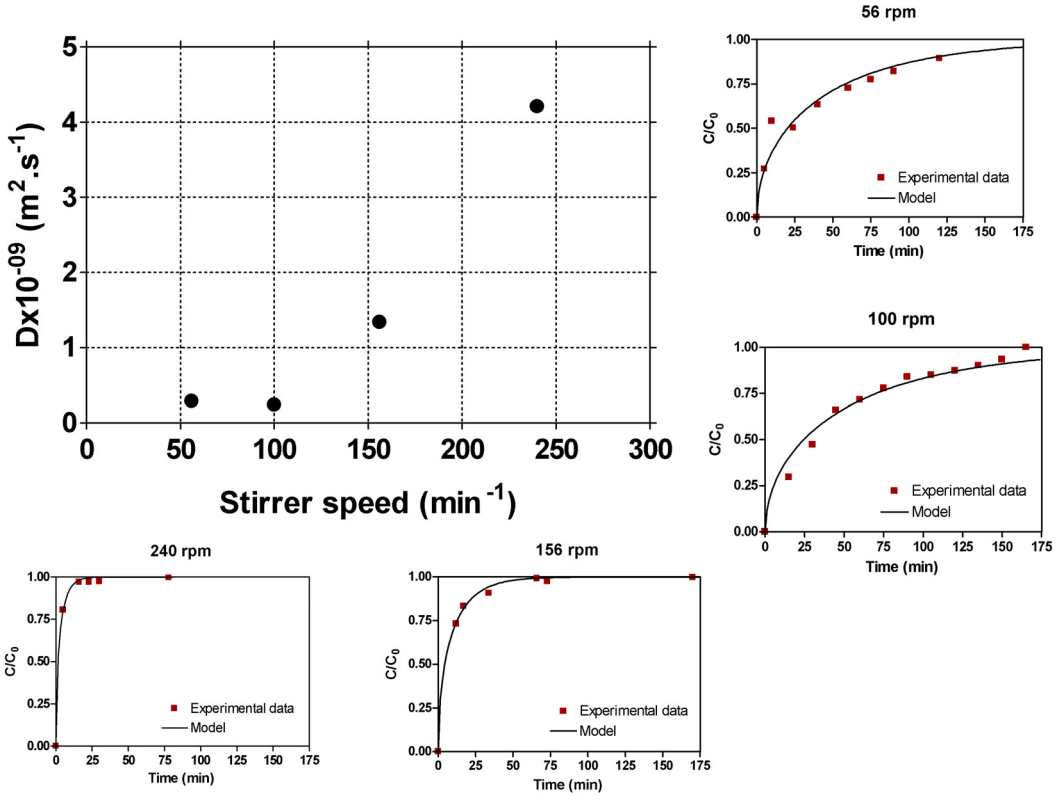

Figure 28 Time dependent up-take of CA onto Type-M resin at different stirrer speed. Initial concentration was 9.0 mg·ml^{-1}.

Stirrer speed (min^{-1})	Experimental D_{pm} ($m^2.s^{-1}$)
56	2.91E-10
100	2.40E-10
156	1.34E-09
240	4.21E-09

Table 9: Experimental diffusion coefficient for Type-M resin.

Overall mass transfer resistance in finite bath

Laboratory contact time experiments were performed in order to obtain concentration decay vs. time curves in a finite bath system. These experimental data was fit by nonlinear correlation methods to appropriate mathematical expressions. At equilibrium, mass transfer, and material balance description of the sorbate-sorbent systems was included in the equations employed. Not only experimental measurements but also theoretical correlations were also used in order to estimate relevant system parameters.

The evidence gathered showed that external mass transfer limitations can be brought to a minimum provided that sufficient mixing exist in the vessel. Appropriate solid and liquid mixing is archived after the Zwietering criteria for particle suspension. As expected, k_f takes a constant value under such experimental conditions. This value for the film side mass transfer coefficient can equally apply to the two types of resin tested since average particle diameters are similar.

A second mass transfer limitation was shown at the intraparticle level. Type-G material, owning to its gel structure, was treated so as to present a homogeneous diffusion type and thus, D_s values were experimentally calculated. Adsorption kinetics of carminic acid on the

gel type material was insensitive to the hydrodynamic condition prevailing in the contactor. This correlates with almost constant mass transfer parameters, both external and internal, as a function of stirrer speed. The only one exception is observed at 56 rpm where the particle suspension was not complete, therefore impacting on product uptake. Overall mass transfer can be further described to have a balance contribution from the film and particle side since value δ was close to 1. The maximum adsorptive performance for the Type-G material was attained in the stirrer contactor operational mode.

On the other hand, the Type-M material showed a more complex behavior. This resin showed increased adsorption performance, as evidence as raising batch uptake kinetic constant ($\boldsymbol{k_1}$) values, as a function of impeller velocities. This was explained in terms of the existence of a bimodal pore structure, which allow for convective transport within the adsorbent beads. This alleviated mass transfer constraints since conventional diffusion into pores takes place alongside shorter distances i.e., shorter diffusion path. In order to account for this phenomenon a modified porous coefficient was defined. The experimental value for $\boldsymbol{D_{pm}}$ at moderate stirrer speed was close to predicted $\boldsymbol{D_p}$ on the basis of theoretical correlations. These values are usually found to be between 3 and 30 times lower than the diffusion coefficient values predicted after the Stokes-Einstein law. On the contrary, in the turbulent regime experimental diffusivities were higher than theoretically expected may be due to the effect of the convective flow. Contribution to overall mass transfer resistances was combined. Calculation of the Biot number showed decreased values as a function of shear stress with correlates with increased particle side diffusion. Again, an exception to this behavior was found when particles were not fully suspended in the vessel. Power delivered to the contactor was limited due to vortex formation. However, the

adsorptive performance of the porous material was close to its maximum as shown by the relation between Biot number and stirrer speed. This was further confirmed employing a spinning basket reactor were despite the intense turbulence created by countercurrent mixing no increased performance was observed (data not shown).

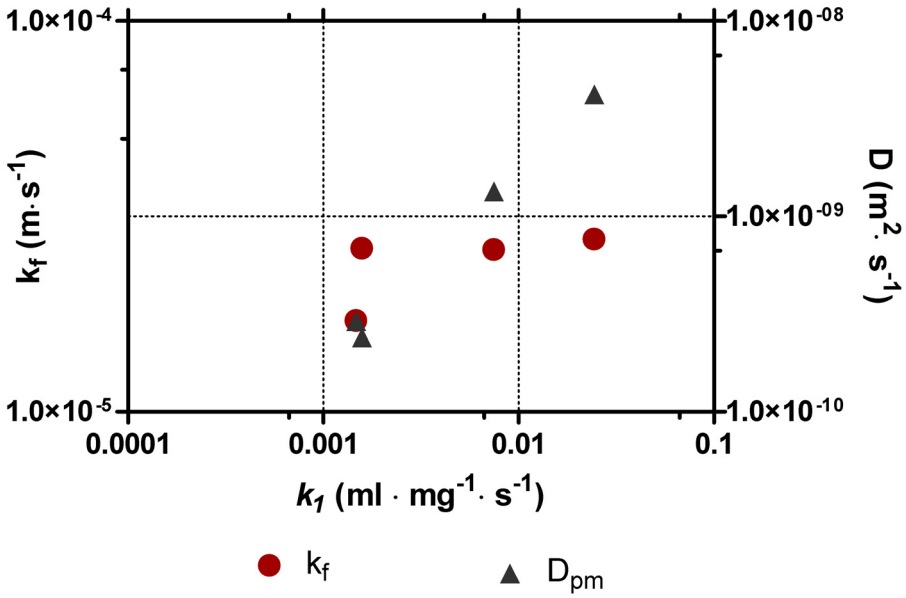

Figure 29: External and internal mass transfer coefficients for the adsorption of carminic acid onto Type-M resin. Experimental kf and Dpm values are plotted as a function of impeller velocity in the contactor.

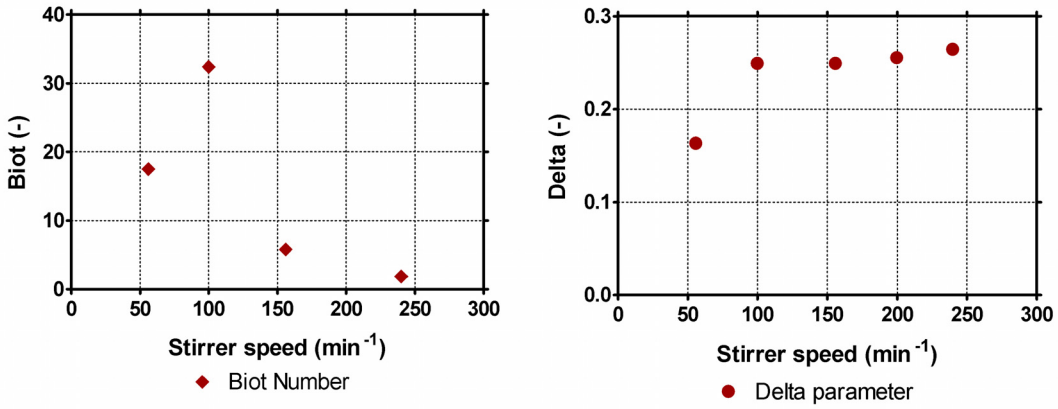

Figure 30: Biot number and delta parameter values as a function of stirrer speed.

4.4. Desorption and further processing

The equilibrium characteristics of carminic acid adsorption on Type-G and Type-M resins were described by a non-linear favorable isotherm of the Langmuir type. These do not necessarily confirmed reversibility. In order to evaluate product desorption form the loaded resins several eluent solutions were tested. The chemical composition of these solutions was designed in order to tackle the various mechanisms, which might participate during solid-product binding. The chemical nature of the materials employed e.g., styrene-divinilbenzene and polyacrylic resins are known to promote hydrophobic and Van der Walls interactions while the charged groups (tertiary amine) can interact with the adsorbate by electrostatic forces. These two mechanisms are present in the resins utilized and therefore they contribute to the observed product binding under operating conditions. A successful desorption strategy would then be able to counteract these binding forces.

Desorption experiments were carried out in an agitated vessel using preloaded solid phase. Composition of the elution solutions included: a) Pure solvents; b) Diluted acid; c) Acid diluted in water / aliphatic alcohol mixtures; d) Solution of hydrophilic polymers or sugars; e) Alkaline solutions with or without added salt. The rationale behind the selection of these chemical components as potential eluting agents was a) increase solubility for carminic acid; b) to protonate carminic acid groups; c) to interfere with both ionic and hydrophobic binding; d) to interfere with other weak interactions and; e) to uncharged the matrix groups or mask the charges, respectively. Figure 31 and Table 10 depict the efficiency of the various eluent mixtures employed. Dilute hydrochloric acid solutions in watery alcohol (methanol, ethanol, or isopropanol) were among the strongest agents in promoting carminic

acid desorption. Further optimization of this mixture lead to the use of half molar acid (final concentration) and alcohol proportions in the range 50-75%, depending on the length of the aliphatic chain (Figure 32). Moreover, a general correlation was found between the total amounts of organic modifier in the mixture and the corresponding desorption strength (Figure 33). This pointed out the importance of simultaneously mask charge mediated and hydrophobic interactions for complete product desorption. In addition, the increased solubility of carminic acid in alcohol at low pH might play a role in the dye recovery. Similar results were showed by other authors describing the use of weak anion exchange resins for the adsorption and subsequent desorption of lactic acid [57, 81]. Additionally, Barboza et.al. (2002) [74], showed that cephalosporin desorption from weak anion exchange resins with ethanol is possible. This author further suggested that ethanol diminishes the strength of the interactions between the cephalosporin molecules and benzene rings in the resin, weakening the adsorption capability.

	Elution Agents	Recovery (%)
A	Water or EtOH	0.00
B	0.5 N HCl	0.37
C	0.5 N HCl + 2% Boric Acid	0.46
D	0.5 N HCl + 75% Methanol	0.87
E	0.5 N HCl + 75% EtOH	0.98
F	0.5 N HCl + 50% Isopropanol	0.95
G	0.5 N HCl + 25% Isop. + 25% EtOH	0.87
H	0.5 N HCl +10% Sucrose	0.37
I	0.5 N HCl + Sorbitol 10 %	0.37
J	0.5 N HCl + 2% PEG (1000)	0.13
K	0.5 N HCl + 2% PVP	0.31
L	1 M NaOH + 1 M NaCl	0.38
M	1 M NH_4OH + 1 M NaCl	0.46
N	0.1 M Potasium hydroxide	0.02
O	0.5 M Potasium hydroxide	0.21
P	1 M Potasium hydroxide	0.33

Isop.: Isopropanol; PVP: Poly-Vinyl-Pyrrolidone; EtOH: Ethanol, MetOH: Methanol; HCl: Hydrochloric acid, PEG: Polyethylene-glycol; NH_4OH: Ammonium hydroxide; NaOH: Sodium hydroxide; NaCl: Sodium chloride

Table 10: Recovery of carminic acid from preloaded adsorbent employing various desorption mixtures.

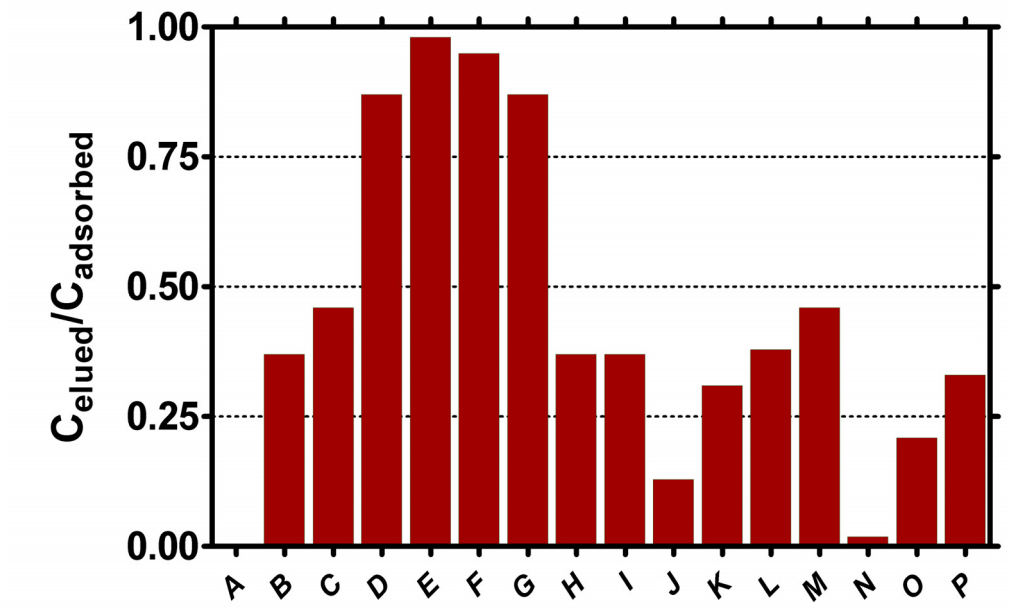

Figure 31: Elution of carminic acid adsorbed upon varying the eluent composition (Table 10).

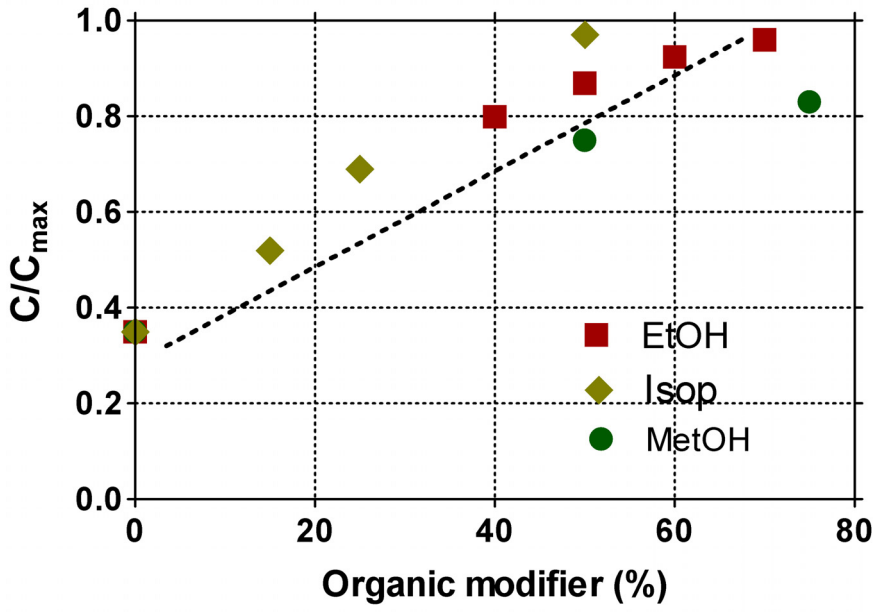

Figure 32: Effect of concentration and of aliphatic chain length on the carminic acid recovery by alcohol mixtures.

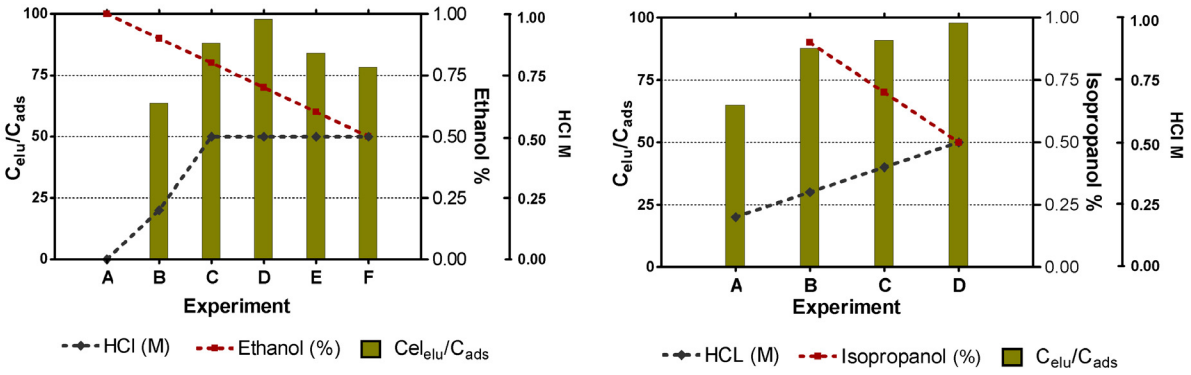

Figure 33: Recovery of carminic acid as function of the composition of dilute acid/ alcohol mixtures.

After selecting an efficient combination of eluting agents an attempt to describe product desorption in more quantitative terms was made. The following equation was found to adequately fit to the experimental data:

$$\frac{C}{C_{\max}} = \frac{R_{\max} \times t}{\tau_{50} + t}$$

Equation 29

Where: C_{max} is the maximum amount of product recoverable, R_{max} is the fraction of maximum recoverable product, and τ_{50} is the time required to release half of the maximum recoverable product. τ_{50} can be use to describe the system. Figure 34 illustrate desorption kinetics of carminic acid from the Type-G material using an optimized elution mixture (0.2 M HCl + 75% EtOH). Kinetics of desorption was mostly relevant at the pilot scale, after product adsorption. Under these conditions both materials Type-G and Type-M performed in a very similar manner. This is an expected result since mass transfer

resistances, as it is known from adsorption design experiments, are comparable as it is the efficiency of the eluent.

Desorbed carminic acid in the acid alcohol-water extract was concentrated by vacuum evaporation. From this step, the organic modifier can be recycled, thus significantly reducing waste generation [81]. The concentrated product was finally formulated as liquid or spray dried to yield a powdered preparation.

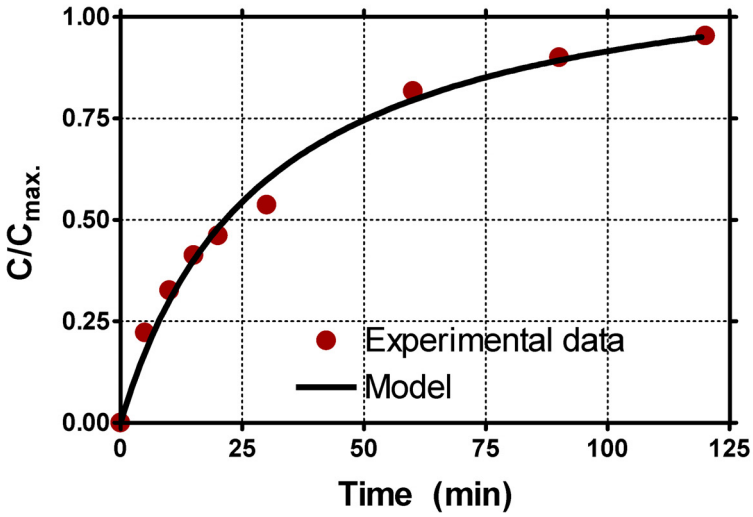

Figure 34: Desorption kinetics of carminic acid.

Final product samples were subjected to chemical and microbiological analysis and found to comply with the *Codex Alimentarius* (FAO and the European Parliament and the Council of European Union). Moreover, allergy testing in rabbits showed no presence of active allergens. Therefore, the product can be regarded as safe for human consumption.

4.5. Process synthesis, pilot scale studies, and scale-up criteria

4.5.1.Total process analysis

Once all carminic acid purification steps were understood in an isolated manner, laboratory scale experiments were performed to access overall process robustness and the resin reusability potential. The cost of the solid matrix is relevant to the global processing cost. Therefore, the number of cycles in which a single adsorbent batch can be employed is a sensitive parameter for further cost analysis. A complete adsorption-desorption process was repeated ten times under optimized conditions without changing the resin (Table 11). Product yield was 85.7 ± 10% on average. This was expected since; product recovery using ion exchangers at laboratory scale is usually in the range 70-85%. However, somewhat reduced recovery rates are usually encountered at larger scales. The process was also tested at the pilot scale in a 0.4 m^3 contactor. Figure 35 shows that global process performance was satisfactory as judged by average yields near 70%. These experiments were used to process 5-15 kg of cochineal with 10-15 kg of adsorbent material. The total time required for a complete cycle (equilibration, adsorption, washing, elution and regeneration) was 6 h. This is 1/10 the time that would be required to run the same adsorption process in the packed-bed mode. Fifty pilot cycles were conducted under not optimized conditions showing that total yields can be actually improved. In conclusion, Type-G and Type-M adsorbents present a favorable behavior for carminic acid recovery, in terms of kinetics, affinity, capacity and susceptibility to regeneration. Further processing to the final product incurred in product loses ≤ 5%. Therefore, total process yields can be well estimated in the range

67-75%, which compares favorably with current process yielding 52% carminic acid from cochineal [17].

4.5.2. Scale-up criteria

On the basis of this work some general recommendations can be made in order to scale-up natural product purification in a batch contactor. The following rules can be applied:

a) Particle suspension is to be assure according to the criteria develop by Zwietering (n_c). Additionally a turbulent regime should be assure by $Re_i > 10^4$. Scale up of the stirred vessel if done on the basis of the geometric similarity and the power number (N_p) method taking into accounts the impeller type and the rheological properties of the fluid.

b) The external mass transfer coefficient (k_f) can be estimated according to Ranz and Marshall [72]. To account for the presence of particulate material of biological origin this value is increased by one order of magnitude.

c) Internal diffusivity (D) must be estimated in accordance to the material employed. For Type-G material a D_s value have to be obtained experimentally and can be assumed to be constant. For Type-M material the *hyperdiffusivity* can be estimated according to this work, as a function of Re_i.

d) The kinetic profile and extent of product uptake in the contactor can be simulated, assuming a rectangular isotherm, employing

the following analytical expression described by Suzuki and Kawazoe (1974) [55]:

$$\tau = \frac{\left(1+\beta^3\right)\left(1+\beta i^{-1}\right)}{3} \ln \frac{\xi^3+\beta^3}{1+\beta^3} + \frac{1+\beta^3}{3\beta} \ln \frac{\xi+\beta}{1+\beta} - \frac{1+\beta^3}{6\beta^3} \quad \textbf{Equation 30}$$

$$\ln \frac{\xi^2-\beta\cdot\xi+\beta^2}{1-\beta+\beta^2} + \frac{1+\beta^3}{\sqrt{3}\cdot\beta}\left\{\tan^{-1}\frac{2-\beta}{\sqrt{3}\cdot\beta} - \tan^{-1}\frac{2\cdot\xi-\beta}{\sqrt{3}\cdot\beta}\right\}$$

Where:

$$\beta = \left(\frac{C_\infty}{C_0 - C_\infty}\right)^{1/3}$$

$$\xi = \left(\frac{C - C_\infty}{C_0 - C_\infty}\right)^{1/3}$$

Bi is the biot number (-); C_0 and C_∞ is the initial and final concentration in the liquid phase ($mg \cdot ml^{-1}$); ***C*** the concentration in the liquid phase ($mg \cdot ml^{-1}$) at the time ***t*** (min.); ρ_p is the particle density ($mg \cdot ml^{-1}$); q^* is the particle concentration in the equilibrium ($g \cdot kg^{-1}$); and D_p is the pore diffusivity ($m^2 \cdot s^{-1}$).

e) Desorption yields are 90% of the total adsorbed product. τ_{50} can be assumed to be the same as for adsorption, as simulated.

	Weigh (g)	Volume (L)	Carminic Acid ($g \cdot ml^{-1}$)	Carminic Acid (kg)	Yield (%) (**)
Cochineal	10			2.10	100
Extraction		0.200	9.90	1.98	94.3
Adsorption		0.200			
Supernatant		0.200	0.53	0.106	
Resin	10			1.874	89.2 (95)
Elution		0.050	34	1.700	
		0.025	4.12	0.1032	
Total Elution		75		1.8032	**85.7** (96)

Table 11: Performance of a typical bench-scale absorptive process for the recovery of carminic acid from cochineal. The raw cochineal contained 21% carminic acid. (**) Refers to the yield of a single step.

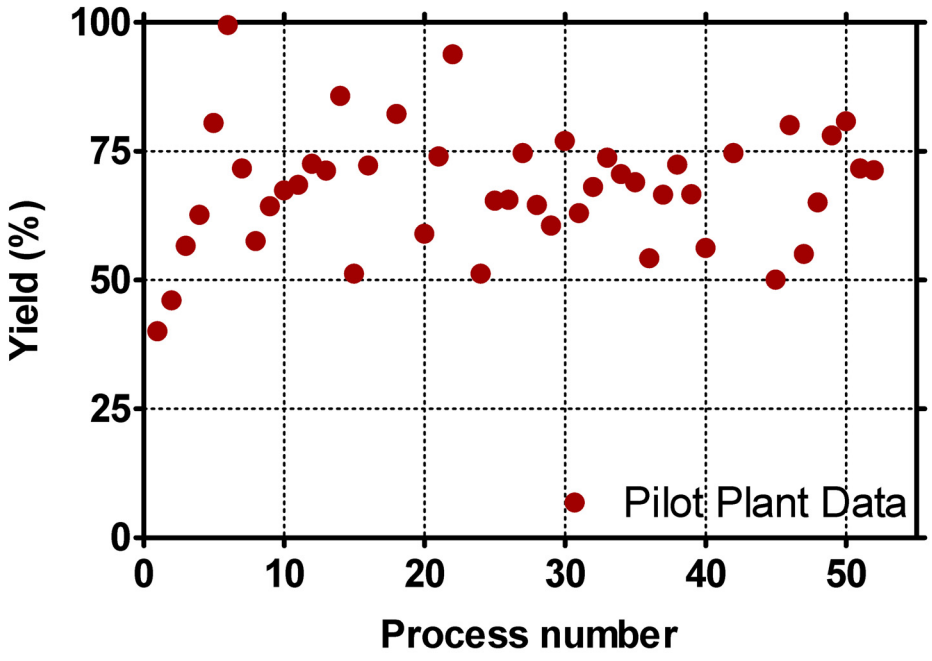

Figure 35: Recovery of carminic acid at pilot-scale. Runs were performed under not optimized conditions.

5. CONCLUSIONS

The recovery and purification of carminic acid from raw cochineal is regarded as a difficult and complicated process. Current industrial processes suffer from low and irreproducible yields while generating a low quality final product. It must be stressed that the overall performance of a purification process, expressed by its overall yield, operation time, and capital cost may contribute to up to 70-90% of the total production costs for a natural or biotechnological product. Therefore, the reduction in the number and the effective integration of unit operations during downstream processing strongly influences the economic competitiveness of a potential product.

The current industrial manufacturing process from cochineal to purified carminic acid was re-examined and re-designed. This was done on the basis of an adsorption process that was able to capture the product directly from crude cochineal extracts even in the presence of biological suspended material. The extraction procedure was also optimized. The whole processing scheme was tested at the laboratory and pilot scales, yielding a product, which conforms to the food industry regulations. Scale-up criteria were developed in order to further transfer the technology to the productive scenario.

The adsorptive process also was able to remove most of the potentially allergenic proteins present in the crude extract when the appropriate resin and operational conditions were chosen. Avoiding lake formation as a means for product precipitation and recovery prevented the use of toxic metallic ions.

After an extensive screening process including ion exchange and hydrophobic interaction solid supports, two anion exchangers were selected from screening experiments. These are bulk available

industrial resins that were named Type-M and Type-G, after their matrix structure. Type-M is a macroporous support while Type-G is gel material.

The equilibrium and dynamic adsorption behavior was study for the adsorbent-carminic acid pairs. The adsorption isotherms were favorable for both materials, which were indicative of a strong dye affinity for the solid phases and both obeyed the Langmuir equation. Maximum capacities ($\boldsymbol{q_m}$) were 250-300 $g \cdot kg^{-1}$ and dissociation constant ($\boldsymbol{K_d}$) were ~ 0.05 $kg \cdot g^{-1}$.

Frontal experiments in packed-bed showed important limitations to mass transfer for the resins employed. Combined mass transfer resistances were described although the particle side component was dominating. Nevertheless, the processing times required for effective product trapping were unacceptable long. In addition, adsorption of carminic acid on packed materials would require previous extensive clarification. This in turn proved to be difficult since cake resistance due to its high compressibility made filtration very difficult. These limitations prompt us to the search of alternative contacting systems: the stirred batch contactor.

Laboratory contact time experiments were performed in order to obtain concentration decay vs. time curves in a finite bath system. These experimental data was fit by nonlinear correlation methods to appropriate mathematical expressions. At equilibrium, mass transfer, and material balance description of the sorbate-sorbent systems was included in the equations employed. Not only experimental measurements but also theoretical correlations were also used in order to estimate relevant system parameters.

The evidence gathered showed that external mass transfer limitations can be brought to a minimum provided that sufficient mixing exist in the contactor. Appropriate solid and liquid mixing is archived after the Zwietering criteria for particle suspension ($\boldsymbol{n_c} > 135$ rpm). As expected, $\boldsymbol{k_f}$ takes a constant value under such experimental conditions (~2.6 E-05 $m \cdot s^{-1}$). This value for the film side mass transfer coefficient can equally apply to the two types of resins tested, since average particle diameters are similar (~700 μm).

A second mass transfer limitation was shown at the intraparticle level. Type-G material, owning to its gel structure, was treated so as to present a homogeneous diffusion type and thus, solid diffusivity ($\boldsymbol{D_s}$) values were experimentally calculated (3.16 E-10 $m^2 \cdot s^{-1}$). Adsorption kinetics of carminic acid on the gel type material was insensitive to the hydrodynamic condition prevailing in the contactor ($4{,}000 < \boldsymbol{Re_i} < 10{,}000$). This correlates with almost constant mass transfer parameters, both external and internal, as a function of stirrer speed. Overall mass transfer can be further described to have a balanced contribution from the film and particle side since value δ was close to 1. Much better sorption performance for the Type-G material was attained in the stirrer contactor operational mode.

On the other hand, the Type-M material showed a more complex behavior. This resin showed increased adsorption performance, as evidence as raising batch uptake kinetic constant ($\boldsymbol{k_1}$) values, as a function of impeller velocities. This was explained in terms of the existence of a bimodal pore structure, which allow for convective transport within the adsorbent beads. In order to account for this phenomenon a modified porous coefficient was defined. The

experimental value for D_{pm} at moderate stirrer speed was close to predicted D_p on the basis of theoretical correlations. On the contrary, in the turbulent regime experimental diffusivities were higher than theoretically expected due to the effect of the convective flow. Contribution to overall mass transfer resistances was combined. Calculation of the Biot number showed decreased values as a function of shear stress with correlates with increased particle side diffusion. Even when power delivered to the contactor was limited due to vortex formation the adsorptive performance of the porous material was close to its maximum as shown by the relation between Biot number and stirrer speed.

After extraction of the cochineal and direct capture onto the resin in the batch contactor elution of the product was accomplished employing dilute hydrochloric acid and ethanol solutions. A general correlation was found between the total amounts of organic modifier in the mixture and the corresponding desorption strength. Desorbed carminic acid in the acid alcohol-water extract was concentrated by vacuum evaporation. The concentrated product was finally formulated as liquid or spray dried to yield a powdered preparation. Total process yields can be well estimated in the range 67-75%, which compares favorably with current process yielding 52% carminic acid from cochineal.

On the basis of this work some general recommendations can be made in order to scale-up natural product purification in a batch contactor. The following rules can be applied:

a) Particle suspension is to be assure according to the criteria develop by Zwietering. Additionally a turbulent regime should be assure by $Re_i > 104$. Scale up of the stirred vessel if done on the

basis of the geometric similarity and the power number ($\boldsymbol{N_p}$) method taking into accounts the impeller type and the rheological properties of the fluid.

b) The external mass transfer coefficient ($\boldsymbol{k_f}$) can be estimated according to Ranz and Marshall. To account for the presence of particulate material of biological origin this value is increased by one order of magnitude.

c) Internal diffusivity ($\boldsymbol{D}$) must be estimated in accordance to the material employed. For Type-G material a $\boldsymbol{D_s}$ value of 3.16E-10 $m^2 \cdot s^{-1}$ can be used for calculations and it is assumed to be constant. For Type-M material the hyperdiffusivity can be estimated according to this work, as a function of $\boldsymbol{Re_i}$.

d) The kinetic profile and extent of product uptake in the contactor can be simulated, assuming a rectangular isotherm, employing the analytical solution provided by Suzuki and Kawazoe (1974).

6. REFERENCES

1. Perez Guerra, G. and M. Kosztarab, *Biosystematics of the family Dactylopiidae (Homoptera: coccinea) with emphasis on the life cycle od Dactylopius coccus Costa*, in *Studies if Morphology and Systematics of Scale Insects*. 1992: Blacksburg, Virginia.
2. Noonan, J., *Color Additives in Food*. 2nd ed, ed. H.o.F. Additives. 1975, Cleveland, Ohio: Furia. 587-615.
3. Downham, A. and P. Collins, *Colouring our foods in the last and next millennium.* International Journal of Food Science and Technology, 2000. **35**(1): p. 5-22.
4. Sloan, A.E., *The natural & organic foods marketplace - Mother nature moves mainstream as the natural and organic foods market grows worldwide.* Food Technology, 2002. **56**(1): p. 27-+.
5. FAO/OMS, *Compendium of Food additive Specifications. Addendum 8.* FAO Food and Nutrition Paper. WHO Technical Report Series No.52 Add. 8, Roma, Italy.2000.
6. Sáenz, C., J. Garrido, and M. Carvallo, *Colorantes Naturales Derivados de la Cochinilla (Dactylopius coccus Costa)*, in *La Alimentacion Latinoamericana*. 2004. p. 56-62.
7. Favaro, G., et al., *Role of protolytic interactions in photo-aging processes of carminic acid and carminic lake in solution and painted layers.* Journal of the Chemical Society-Perkin Transactions 2, 2002(1): p. 192-197.
8. Gonzalez, M., et al., *Optimizing conditions for the extraction of pigments in cochineals (Dactylopius coccus Costa) using response surface methodology.* J Agric Food Chem, 2002. **50**(24): p. 6968-74.
9. Lloyd, A.G., *Extraction and Chemistry of Cochineal.* Food Chemistry, 1980. **5**(1): p. 91-107.
10. BARYANYOVITS, F.L.C., *Cochineal carmine: an ancient dye with a modern role.* Endeavour (New Series), 1978. **2 (2)**: p. 85-92.
11. Eisner, T., et al., *Defensive use of an acquired substance (carminic acid) by predaceous insect larvae.* Experientia, 1994. **50**(6): p. 610-5.
12. Edmonds, J., *The History and Practice of Eighteenth Century Dyeing*, in *Historic Dyes Series*. 1999.

13. Rodriguez, L.C., M.A. Mendez, and H.M. Niemeyer, *Direction of dispersion of cochineal (Dactylopius coccus Costa) within the Americas.* Antiquity, 2001. **75**: p. 73-77.
14. Flores, V. *Cosecha y postcosecha de cochinilla en la sierra del Peru.* in *Anales: I Seminario Internacional de la Cochinilla*. 1996. Ayacicho, Peru.
15. Perez, J., *Anteproyecto de una planta procesadora de grana de cochinilla para la obtencion de sus principales derivados: extracto de cochinilla, carmin de cochinilla y acido carminico*, in *Escuela de Quimica*. 1992, Universidad de La Salle: Mexico. p. 137.
16. Cabrera, R. and H.M. Fernandez-Lahore, *Downstream Processing de productos naturales: Recuperación y purificación del ácido carmínico como aditivo en la industria alimentaria, farmacéutica y cosmética.*, C.R.D. Report, Editor. 2001, ANPCyT (FONTAR-ANR NA127): Buenos Aires.
17. IDRC, *Carmin Extraction Technology*. 1999, International Development Research Center.
18. en_1995L0045_do_001.pdf, h.e.e.i.e.-l.e.c.p., *CONSLEG 1995L0045-10/05/2004*. 2004, Official Publications of the European Communities.
19. Chung, K., et al., *Identification of carmine allergens among three carmine allergy patients.* Allergy, 2001. **56**(1): p. 73-7.
20. Acero, S., et al., *Occupational asthma and food allergy due to carmine.* Allergy, 1998. **53**(9): p. 897-901.
21. Beaudouin, E., et al., *Food anaphylaxis following ingestion of carmine.* Ann Allergy Asthma Immunol, 1995. **74**(5): p. 427-30.
22. Aquino, G. and N. Barcenas. *Cria de la cochinilla para la prodruccion de grana y sus posibilidades de resurgimiento en Mexico.* in *Memorias del VIII Congreso Nacional y VI Internacional sobre el aprovechamiento del Nopal.* 1999. Peru: Union Autonoma de San Luis Potosi, Inst. de Investigacion de Zonas Deserticas.
23. Sugimoto, N., et al., *Structure of acid-stable carmine.* Journal of the Food Hygienic Society of Japan, 2002. **43**(1): p. 18-23.

24. Mendez, J., et al., *Color quality of pigments in cochineals (Dactylopius coccus Costa). Geographical origin characterization using multivariate statistical analysis.* J Agric Food Chem, 2004. **52**(5): p. 1331-7.
25. Verrall, M.S., *Downstream processing of natural products : a practical handbook*. 1996, Chichester ; New York: J. Wiley. xviii, 354.
26. Gluszcz, P., et al., *Equilibrium and dynamic investigations of organic acids adsorption onto ion-exchange resins.* Bioprocess and Biosystems Engineering, 2004. **26**(3): p. 185-190.
27. Thommes, J., *Fluidized Bed Adsorption as a Primary Recovery Step in Protein Purification.* Advances in Biochemical Engineering/ Biotechnology, 1997. **58**: p. 185-230.
28. Lyddiatt, A., *Process chromatography: current constraints and future options for the adsorptive recovery of bioproducts.* Current Opinion in Biotechnology, 2002. **13**(2): p. 95-103.
29. Doran, P.M., *Bioprocess Engineering Principles*. seventh ed, ed. A. Press. 2002.
30. Mccoy, M.A. and A.I. Liapis, *Evaluation of Kinetic-Models for Biospecific Adsorption and Its Implications for Finite Bath and Column Performance.* Journal of Chromatography, 1991. **548**(1-2): p. 25-60.
31. Bradford, M.M., *Rapid and Sensitive Method for Quantitation of Microgram Quantities of Protein Utilizing Principle of Protein-Dye Binding.* Analytical Biochemistry, 1976. **72**(1-2): p. 248-254.
32. Skoog, D.A., F.J. Holler, and T.A. Nieman, *Principles of instrumental analysis*. 5 ed, ed. P.S.C. Pub. 1988, Orlando, Fla.: Harcourt Brace College Publishers, c1998.
33. AOAC, *Association of Analytical Communities*. www.AOAC.org.
34. del Canizo, A.A.N., et al., *Acid protease purification by dye affinity chromatography.* Afinidad, 2001. **58**(493): p. 231-233.
35. Scopes, R.K., *Protein purification : principles and practice*. 3rd ed. Springer advanced texts in chemistry. 1994, New York: Springer-Verlag. xix, 380.

36. Skidmore, G.L., B.J. Horstmann, and H.A. Chase, *Modeling Single-Component Protein Adsorption to the Cation Exchanger S Sepharose Ff.* Journal of Chromatography, 1990. **498**(1): p. 113-128.
37. Miranda, M.V., et al., *Optimisation of peroxidase adsorption on concanavalin A-agarose.* Latin American Applied Research, 2003. **33**(2): p. 67-71.
38. Yamamoto, S. and Y. Sano, *Short-Cut Method for Predicting the Productivity of Affinity-Chromatography.* Journal of Chromatography, 1992. **597**(1-2): p. 173-179.
39. Fernandez-Lahore, H.M., et al., *The influence of cell adsorbent interactions on protein adsorption in expanded beds.* Journal of Chromatography A, 2000. **873**(2): p. 195-208.
40. Hall, K.R., et al., *Pore- and Solid-Diffusion Kinetics in Fixed-Bed Adsorption under Constant-Pattern Conditions.* Industrial & Engineering Chemistry Fundamentals, 1966. **5**(2): p. 212-&.
41. Watanabe, T. and S. Terabe, *Analysis of natural food pigments by capillary electrophoresis.* Journal of Chromatography A, 2000. **880**(1-2): p. 311-322.
42. Lancaster, F.E. and J.F. Lawrence, *High-performance liquid chromatographic separation of carminic acid, alpha- and beta-bixin, and alpha- and beta-norbixin, and the determination of carminic acid in foods.* Journal of Chromatography A, 1996. **732**(2): p. 394-398.
43. Merino, L., U. Edberg, and H. Tidriks, *Development and validation of a quantitative method for determination of carmine (E120) in foodstuffs by liquid chromatography: NMKL1 collaborative study.* Journal of Aoac International, 1997. **80**(5): p. 1044-1051.
44. Berzas-Nevado, J.J., C. Guiberteau-Cabanillas, and A.M. Contento-Salcedo, *A reverse phase HPLC method to determine six food dyes using buffered mobile phase.* Analytical Letters, 1998. **31**(14): p. 2513-2535.
45. Maier, M.S., S.D. Parera, and A.M. Seldes, *Matrix-assisted laser desorption and electrospray ionization mass spectrometry of carminic acid*

isolated from cochineal. International Journal of Mass Spectrometry, 2004. **232**(3): p. 225-229.

46. Andrzejewska, E., *[Detection of a natural organic dye, cochineal, in meat products].* Rocz Panstw Zakl Hig, 1981. **32**(4): p. 315-8.
47. Carvalho, P.R.N. and C.H. Collins, *HPLC determination of carminic acid in foodstuffs and beverages using diode array and fluorescence detection.* Chromatographia, 1997. **45**: p. 63-66.
48. Panadero, S., A. GomezHens, and D. PerezBendito, *Kinetic determination of carminic acid by its inhibition of lanthanide sensitized luminescence.* Fresenius Journal of Analytical Chemistry, 1997. **357**(1): p. 80-83.
49. Yoshida, A., Y. Takagaki, and T. Nishimune, *Enzyme-Immunoassay for Carminic Acid in Foods.* Journal of Aoac International, 1995. **78**(3): p. 807-811.
50. Motulsky, h.j., *GraphPad Prism Version 4.0 Statistics Guide - Statistical analyses for laboratory and clinical reserchers.*, G.S. Inc., Editor. 2003: San Diego, CA.
51. Ziegler, R., et al., *A new type of highly polymerized yolk protein from the cochineal insect Dactylopius confusus.* Archives of Insect Biochemistry and Physiology, 1996. **31**(3): p. 273-287.
52. Bartels, C., et al., *A. novel ion-exchange method for the isolation of streptomycin.* Chem. Eng. Progr, 1958. **54**: p. 49.
53. Chang, C. and A.M. Lenhoff, *Comparison of protein adsorption isotherms and uptake rates in preparative cation-exchange materials.* Journal of Chromatography A, 1998. **827**(2): p. 281-293.
54. Belter, P.A., E.L. Cussler, and W. Hu, *Downstream Processing for Biotechnology.* Bioseparation, 1988. **6**: p. 145-179.
55. Suzuki, M., *Adsorption Engineering*, in *Chemical Engineering Monographs - Adsorption Engineering*, E.S.P. B.V., Editor. 1990.
56. Wong, Y.C., et al., *Adsorption of acid dyes on chitosan-equilibrium isotherm analyses.* Process Biochemestry, 2004. **39**: p. 693-702.
57. Moldes, A.B., J.L. Alonso, and J.C. Parajo, *Recovery of lactic acid from simultaneous saccharification and fermentation media using anion*

exchange resins. Bioprocess and Biosystems Engineering, 2003. **25**(6): p. 357-363.

58. Cao, X.J., H.S. Yun, and Y.M. Koo, *Recovery of L-(+)-lactic acid by anion exchange resin Amberlite IRA-400.* Biochemical Engineering Journal, 2002. **11**(2-3): p. 189-196.
59. Chen, B., C.W. Hui, and G. McKay, *Film-pore diffusion modeling and contact time optimization for the adsorption of dyestuffs on pith.* Chemical Engineering Journual, 2001. **84**: p. 77-94.
60. Ruthven, D.M., *Principles of Adsorption and Adsorption Processes*. 1984: John Wiley & Sons.
61. Foo, S.C. and R.G. Rice, *Prediction of Ultimate Separation in Parametric Pumps.* Aiche Journal, 1975. **21**(6): p. 1149-1158.
62. Guiochon, G., S.G. Shirazi, and A.M. Katti, *Fundamentals of preparative and nonlinear chromatography*. 1994, Boston: Academic Press. xv, 701.
63. Arve, B.H. and A.I. Liapis, *Modeling and Analysis of Biospecific Adsorption in a Finite Bath.* Aiche Journal, 1987. **33**(2): p. 179-193.
64. Choy, K.K.H., J.F. Porter, and G. McKay, *Film-pore diffusion models - analytical and numerical solutions.* Chemical Engineering Science, 2004. **59**(3): p. 501-512.
65. Meshko, V., et al., *Adsorption of basic dyes on granular acivated carbon and natural zeolite.* Water Research, 2001. **35**(14): p. 3357-3366.
66. Ma, Z., R.D. Whitley, and N.H.L. Wang, *Pore and surface diffusion in multicomponent adsorption and liquid chromatography systems.* Aiche Journal, 1996. **42**(5): p. 1244-1262.
67. Fernandez, M.A. and G. Carta, *Characterization of protein adsorption by composite silica-polyacrylamide gel anion exchangers .1. Equilibrium and mass transfer in agitated contactors.* Journal of Chromatography A, 1996. **746**(2): p. 169-183.
68. Atun, G. and G. Hisarli, *Adsorption of carminic acid, a dye onto glass powder.* Chemical Engineering Journal, 2003. **95**(1-3): p. 241-249.
69. Perry, R.H., *Perry's Chemical Engineer's Handbook*. seventh edition ed, ed. D.W. Green. 1997: McGranw-Hill.

70. Zwietering, T.N., *Suspending of Solid Particles in Liquid by Agitators.* Chemical Engineering Science, 1958. **8**(3-4): p. 244-253.
71. Kaufman, E.N., S.P. Cooper, and B.H. Davison, *Screening of Resins for Use in a Biparticle Fluidized-Bed Bioreactor for the Continuous Fermentation and Separation of Lactic-Acid.* Applied Biochemistry and Biotechnology, 1994. **45-6**: p. 545-554.
72. Ranz, W.E. and W.R. Marshall, *Evaporation from Drops .1.* Chemical Engineering Progress, 1952. **48**(3): p. 141-146.
73. Boyd, G.E., A.W. Adamson, and L.S. Myers, *The Exchange Adsorption of Ions from Aqueous Solutions by Organic Zeolites .2.* Journal of the American Chemical Society, 1947. **69**(11): p. 2836-2848.
74. Barboza, M., C.O. Hokka, and F. Maugeri, *Continuous cephalosporin C purification: dynamic modelling and parameter validation.* Bioprocess and Biosystems Engineering, 2002. **25**(3): p. 193-203.
75. Misic, D.M., et al., *Liquid-to-Particle Mass-Transfer in a Stirred Batch Adsorption Tank with Non-Linear Isotherm.* Journal of Chemical Engineering of Japan, 1982. **15**(1): p. 67-70.
76. Helfferich, F. and M.S. Plesset, *Ion Exchange Kinetics - Nonlinear Diffusion Problem.* Journal of Chemical Physics, 1958. **28**(3): p. 418-424.
77. Slater, M.J., *Batch Processes*, in *Principles of Ion Exchange Technology*. 1991, Butterworth-Heinemann.
78. Kirkland, J.J., *2nd International-Symposium on Column Liquid-Chromatography, Wilmington, Del (USA), May 17-19, 1976 - Foreword.* Journal of Chromatography, 1976. **125**(1): p. 1-1.
79. Van Kreveld, M.E. and N. Van den Hoed, *Mass transfer phenomena in gel permeation chromatography.* Journal of Chromatography A, 1978. **1949**: p. 71-91.
80. Frey, D.D., E. Schweinheim, and C. Horvath, *Effect of Intraparticle Convection on the Chromatography of Biomacromolecules.* Biotechnology Progress, 1993. **9**(3): p. 273-284.

81. Evangelista, R.L. and Z.L. Nikolov, *Recovery and purification of lactic acid from fermentation broth by adsorption.* Applied Biochemistry and Biotechnology, 1996. **57-8**: p. 471-480.